Follicular helper- and peripheral helper-like T cells drive autoimmune disease in human immune system mice

Mohsen Khosravi-Maharlooei*[1,2], Andrea Vecchione*[1, 3], Nichole Danzl[1], Hao Wei Li[1], Grace Nauman[1,4], Rachel Madley[1,4], Elizabeth Waffarn[1], Robert Winchester[1], Amanda Ruiz[1], Xiaolan Ding[1], Georgia Fousteri[3], Megan Sykes[1,4,5]

[1] Columbia Center for Translational Immunology, Department of Medicine, Columbia University Medical Center, Columbia University, New York, New York, USA.

[2] Department of Immunology, Department of Biochemistry and Molecular Biology, Mayo Clinic, Phoenix, AZ, USA.

[3] San Raffaele Hospital, Milan, Italy.

[4] Department of Microbiology and Immunology, Columbia University Medical Center, Columbia University, New York, New York, USA.

[5] Department of Surgery, Columbia University Medical Center, Columbia University, New York, New York, USA.

* These authors contributed equally.

Correspondence: Megan Sykes, megan.sykes@columbia.edu

ABSTRACT

Human immune system (HIS) mice constructed in various ways are widely used for investigations of human immune responses to pathogens, transplants and immunotherapies. In HIS mice that generate T cells *de novo* from hematopoietic progenitors, T cell-dependent multisystem autoimmune disease occurs, most rapidly when the human T cells develop in the native NOD.Cg-*Prkdc*^{scid} *Il2rg*^{tm1Wjl} (NSG) mouse thymus, where negative selection is abnormal. Disease develops very late when human T cells develop in human fetal thymus grafts, where robust negative selection is observed. We demonstrate here that PD-1^{+}CD4^{+} peripheral (Tph) helper-like and follicular (Tfh) helper-like T cells developing in HIS mice can induce autoimmune disease. Tfh-like cells were more prominent in HIS mice with a mouse thymus, in which the highest levels of IgG were detected in plasma, compared to those with a human thymus. While circulating IgG and IgM antibodies were autoreactive to multiple mouse antigens, in vivo depletion of B cells and antibodies did not delay the development of autoimmune disease. Conversely, adoptive transfer of enriched Tfh- or Tph-like cells induced disease and autoimmunity-associated B cell phenotypes in recipient mice containing autologous human APCs without T cells. Tfh/Tph cells from mice with a human thymus expanded and induced disease more rapidly than those originating in a murine thymus, implicating HLA-restricted T cell-APC interactions in this process. Since Tfh, Tph, autoantibodies and lymphopenia-induced proliferation (LIP) have all been implicated in various forms of human autoimmune disease, the observations here provide a platform for the further dissection of human autoimmune disease mechanisms and therapies.

Introduction

Human immune system (HIS) mice provide unique opportunities to investigate human immune biology and therapies. Many different versions of these models exist, the simplest of which involves infusion of human lymphocytes from human donors into immunodeficient mouse recipients. Such models, however, are limited by graft-vs-host disease (GVHD) initiated by adoptively transferred human xenoreactive T cells that recognize murine host antigens, thereby limiting the duration and type of information that can be obtained from such models. Additional HIS mouse models involve the *de novo* generation in immunodeficient mouse recipients of human immune systems from human hematopoietic stem and progenitor cells injected intravenously. When NOD mice deficient in T, B and NK cells such as NOD.Cg-*Prkdc*^{scid} *Il2rg*^{tm1Wjl} (NSG) mice are used as recipients, human T cells develop in the murine thymus, while B cells and myeloid antigen-presenting cells develop in the recipient bone marrow. However, we recently demonstrated that human T cells developing *de novo* in the NSG mouse thymus do not undergo normal negative selection for self-antigens and lack normal thymocyte diversity. We further showed that the thymus does not develop normal structure and contains a paucity of medullary epithelial cells. These T cells induce a multiorgan disease characterized by human immune cell infiltrates in multiple organs, usually within 5-8 months after transplantation[1]. Because the causal T cells develop *de novo* in the recipient mice, we describe this as an autoimmune disease rather than graft-vs-host disease (GVHD), which is induced by mature T cells transferred to immunodeficient mice in human hematopoietic cell grafts[2]. The slowly-evolving autoimmune disease induced by T cells developing *de novo* in the murine host is independent of direct recognition of murine antigens, as it develops with similar velocity in NSG mice expressing murine MHC and those completely lacking murine Class I and Class II MHC antigens[1]. Another model involves the transplantation

of an autologous or partially HLA- matched (to intravenously administered fetal $CD34^+$ cells) human fetal thymus graft, in which T cells develop. In this case, the developing thymocytes undergo negative selection for self antigens[1], reflecting the presence of both human and murine[3] APCs in the thymus graft and the presence of a normal human cortico-medullary thymic structure[1]. T cells developing in a human thymus graft eventually cause autoimmune disease, but with a significant delay if the native murine thymus has been removed[1].

The original descriptions of this model involved the use of human fetal thymus and liver tissue engrafted under the kidney capsule along with intravenous administration of $CD34^+$ cells from the same fetal liver[4-6]. While the term "bone marrow, liver, thymus, BLT" mouse has been widely used to describe this model, the model does not include bone marrow and we found the fetal liver fragment to be unnecessary for immune system development. Consequently, "BLT" does not adequately describe the essential components of the model. Instead, we have adopted the term "Hu/Hu" to denote HIS mice constructed with human (Hu) fetal thymus and autologous human fetal liver $CD34^+$ cells administered i.v[7]. Denoting the origin of the thymus and $CD34^+$ cells separately has allowed us to specify variations on the model in which, for example, the thymus tissue originates in fetal swine (the "Sw/Hu" model[8-11]) or when the native mouse thymus is used to generate human T cells (the "Mu/Hu" model described here)[7].

We have now examined the role of B cells, autoantibodies and T cell help for B cells in the development of autoimmune disease in HIS mice. Our results demonstrate that B cell help from follicular (Tfh)- and peripheral (Tph) helper-like T cells drives B cell differentiation and autoantibody responses and that these T cells are sufficient to cause disease in the absence of B cells or antibodies. Furthermore, a global lack of T cell tolerance to murine and human self

antigens is a major driver of autoimmune disease among HIS mice whose T cells develop in a murine thymus. In contrast, the disease that develops later in HIS mice whose T cells develop in a human thymus is likely dependent on a lack of tolerance to tissue-restricted murine antigens presented on human APCs. These studies provide novel insights with utility for dissecting mechanisms of autoimmune disease induction by human T cells.

Results

Mouse-reactive T cells in HIS mice with mouse or human thymus

We have previously demonstrated that a thymus-dependent multi-organ autoimmune disease occurs in HIS mice generated by intravenous injection of human fetal liver (FL) $CD34^+$ cells into NSG mice and that this disease develops more rapidly in mice containing a native murine thymus (termed "Mu/Hu mice" [murine thymus/human $CD34^+$ cells]) than in thymectomized[12] NSG mice receiving a human thymus graft, termed "Hu/Hu mice" (human thymus/human $CD34^+$ cells)[1]. While Mu/Hu mice rely on the native mouse thymus for human T cell development, T cells in Hu/Hu mice develop in the human fetal thymus graft. At 20 weeks after transplantation, animals in both groups were sacrificed and their splenocytes were CFSE-labeled and tested for reactivity to autologous FL-derived human dendritic cells (DCs) and for responses to NSG mouse bone marrow-derived DCs (anti-host response) as well as responses to autologous human DCs pulsed with apoptotic NSG mouse DCs (indirect anti-host response). As shown in Fig. 1A-B, T cells from Hu/Hu and Mu/Hu mice showed proliferation to autologous human DCs that was not significantly augmented by pulsing of human DCs with murine antigens. Since the responder splenocyte preparations were not depleted of murine cells, we cannot distinguish

whether the baseline proliferation represents responses to human antigens or to murine antigens presented by these DCs. However, proliferation of both CD4 and CD8 T cells to NSG mouse DCs was greater in Mu/Hu mice than in 3 of 4 Hu/Hu mice, which showed little, if any, direct proliferation to murine antigens. Proliferation of Mu/Hu $CD4^+$ T cells to murine DCs was significantly greater than proliferation in the absence of DCs, in contrast to Hu/Hu CD4 cells, suggesting a lack of tolerance to NSG antigens only in Mu/Hu $CD4^+$ T cells (Fig. 1B). This observation is consistent with the lack of cortico-medullary structure or normal negative selection in the native murine thymi[1].

Increased number of Tfh cells in HIS mice with a mouse thymus compared to those with a human thymus

Since increases in Tfh and Tph have been associated with various human autoimmune diseases, we compared Tfh-like and Tph-like cells in groups of Mu/Hu ($n = 8$) and Hu/Hu mice ($n = 11$) generated from the same two FL donors (Fig. 2A). $CD3^+$ T cells were detected in peripheral blood around 12 weeks after transplantation (data not shown), as we previously reported[1,3,12].

We monitored PD-1^+CXCR5^- Tph-like and PD-1^+CXCR5^+ Tfh-like $CD4^+$CD45RA^- T cell reconstitution from 12 to 32 weeks post transplantation (Fig. 2B-D). Circulating Tph-like cells were detected at 13 weeks post-transplantation in both groups. The frequency and absolute numbers of Tph-like cells in blood of Mu/Hu mice tended to be greater than those in Hu/Hu mice and the difference in percentages achieved statistical significance across multiple time points (Fig. 2C). Circulating Tfh-like cells appeared at 13 weeks post-transplantation in Mu/Hu mice (Fig. 2D), increased progressively over time and were significantly more abundant in this group than in Hu/Hu mice (Fig. 2D).

In additional experiments, we compared splenic Tfh-like and Tph-like cells in Mu/Hu (*n = 19*) and Hu/Hu mice (*n = 29*) (*n = 5* different FL donors) sacrificed before 20 weeks, between 20-30 weeks and more than 30 weeks post-CD34$^+$ FL transplantation (Fig. 2E). While no significant differences in Tph-like cell frequency and absolute numbers were detected between the two groups (Fig. 2F), percentages of Tfh-like cells were significantly greater in spleens of Mu/Hu compared to Hu/Hu mice (Fig. 2G). The numbers of both Tph-like and Tfh-like cells increased over time in both HIS mouse groups and staining for Ki67 revealed high proliferative rates for both cell types (Fig. S1).

These results suggest that Tph and Tfh differentiate and expand over time and do so more rapidly in Mu/Hu than Hu/Hu mice. These data correlate with the more rapid onset of autoimmune disease in Mu/Hu than Hu/Hu mice, consistent with a role for these T cell types in disease development.

To further characterize Tph-like and Tfh-like cells in HIS mice, we measured ICOS expression and IL-21 production (Fig. 2H-I) . These cells expressed higher levels of ICOS (Fig. 2H) and, upon phorbol myristic acid (PMA)/ionomycin stimulation, secreted more IL-21 (Fig. 2I) compared to control, CD45RA$^+$ T cells, consistent with helper function and with their role in humans. The majority of Tfh-like and Tph-like cells in Mu/Hu and Hu/Hu mice expressed ICOS, though the percentage of ICOS$^+$ cells was significantly higher in Mu/Hu Tfh-like and Tph-like cells compared to their Hu/Hu counterparts (Fig. 2J).

We also compared the levels of FOXP3 within splenic Tfh-like and Tph-like populations in Hu/Hu and Mu/Hu mice. Approximately 10% of Tfh-like and Tph-like cells in both Hu/Hu and Mu/Hu groups were FOXP3$^+$, with the highest proportion observed in Hu/Hu Tph-like cells (Fig. 2K).

Increased serum IgG in Mu/Hu compared to Hu/Hu HIS mice

To determine whether or not the increased proportion of Tfh-like cells in Mu/Hu HIS mice impacted B cell differentiation and survival, as reported in humans[12], we monitored total B cell reconstitution and serum IgM and IgG levels over time. While overall B cell reconstitution (Fig. 3A) and serum IgM concentration was similar between Mu/Hu and Hu/Hu mice, serum IgG levels were significantly greater in Mu/Hu mice (Fig. 3B), suggesting increased B cell differentiation and IgG class switching.

Helper function of Tfh and Tph in Mu/Hu and Hu/Hu mice

Next, to compare the functional capacity of Tfh-like and Tph-like cells from HIS mice with mouse or human thymus, we measured the ability of sorted $CD25^{-}CXCR5^{+}$ $CD45RA^{-}$ (including Tfh and excluding regulatory follicular cells) and $CD25^{-}$ $CXCR5^{-}CD45RA^{-}$ (including Tph cells and excluding Tregs) $CD4^{+}$ cells to induce differentiation of $CD19^{+}CD38^{-}IgD^{+}CD27^{-}$ naïve B cells to $CD20^{-}CD38^{+}$ plasmablasts *in vitro* (Fig. 3C). After isolation, these T cell fractions were incubated with autologous naïve B cells. Helper cells from both Mu/Hu and Hu/Hu mice induced plasmablast formation and this activity was greater at later (>20 weeks) than earlier (<20 weeks) times post-transplant. However, Tfh-like cells from Hu/Hu mice demonstrated greater B cell helper function than those from Mu/Hu mice, particularly in the later time period. A similar trend was seen for Tph-like cells (Fig. 3D), indicating that T-B cell interactions are more effective for T cells generated in a human thymus that is isogenic to the B cells than for those generated in a xenogeneic murine thymus, and consistent with previous literature[14-16].

Because B cells undergo class switching in germinal centers (GC), whose activity can be estimated by plasma CXCL13 levels, we analyzed serum concentrations of human CXCL13 in HIS mice. While human CXCL13 was detected in both groups and did not correlate with the number of splenic Tfh or Tph cells (data not shown), the levels tended to be higher in Mu/Hu compared to Hu/Hu mice (Fig. 3E).

Splenic B cell follicles and germinal centers in HIS mice

We performed histological and immunostaining analyses of spleens to quantify B cell follicles in tissue sections from Mu/Hu (n = 8) and Hu/Hu (n = 11) mice at three time points (<20 weeks, 20–30 weeks, and >30 weeks post-transplantation). Tissue sections were stained for CD3 (T cells), CD20 (B cells), and peanut agglutinin (PNA, marking GC-B cells) (Fig. 4A). B cell follicles were manually quantified, and their size (in pixels per area) was determined using ImageJ software.

H&E staining revealed a semi-organized splenic structure, with distinct B and T cell localization and well-defined follicles up to 30 weeks post-transplant in both groups. However, after 30 weeks, spleens showed fewer B cell follicles and appeared disorganized (Fig. 4B-C). Three-color immunofluorescence staining on spleens from 4 Hu/Hu and 3 Mu/Hu mice at <20 weeks post-transplant revealed distinct B cell areas ($CD20^+$), with PNA^+ cells concentrated within B cell zones but also distributed in other splenic regions. Analysis of spleens from 4 Hu/Hu and 3 Mu/Hu mice at 20–30 weeks post-transplant revealed smaller B cell zones compared to earlier time points, and PNA^+ cells were dispersed throughout the spleen rather than being enriched in B cell areas. Only 2 Mu/Hu mice showed clear B cell zones with localized PNA^+ areas. Beyond 30 weeks post-transplant, spleens from 2 Hu/Hu and 2 Mu/Hu mice revealed no distinct B cell zones, and PNA^+

cells were diffusely distributed.

Despite the increased number of Tfh-like cells in the spleens of Mu/Hu mice, there were no significant differences in the number or total area of splenic follicles between Mu/Hu and Hu/Hu mice (Fig.4B).

Autoreactivity of IgM and IgG in HIS mice

To investigate the possible role of autoantibodies in driving autoimmune disease in HIS mice, we tested serum IgG and IgM for autoreactivity (Fig.5). Fig. 5B confirms, in a separate experiment from that in Fig. 3, a progressive increase in total serum IgM levels in both groups over time, while Fig. 5D shows high levels of IgG antibodies in sera of Mu/Hu mice already by 20 weeks, when Hu/Hu mice still showed very low IgG levels. As shown in Fig. 5A and Table 1, serum from Mu/Hu and Hu/Hu mice contained IgM antibodies that were reactive to multiple murine tissues. Several Mu/Hu mice also contained IgG antibodies with broad reactivity to multiple murine tissues. IgM in sera from HIS mice was reactive to LPS, insulin and dsDNA, and these levels increased over time irrespective of the thymus type (Fig. 5C). IgG against these antigens also increased over time in both groups (Fig. 5E), even though total IgG levels tended to be higher in Mu/Hu than Hu/Hu mice (Fig. 5D). To assess the possibility that IgM autoantibodies might be polyreactive, we compared the sum of IgM concentrations reacting to dsDNA, insulin and LPS to total serum IgM concentrations and observed that the sum of these reactivities was >100% for 3 Mu/Hu mice (Fig. 5F), consistent with polyreactivity of individual B cells in these mice.

Depletion of B cells does not impact development of autoimmunity

To link the B cell types in HIS mice with autoantibody production, we performed phenotypic analysis of B cells. These studies revealed increased proportions of activated or age-associated B cells ($IgD^{-}CD27^{+}CD11c^{+}$) and atypical B cells ($IgD^{-}CD27^{-}CD11c^{+}$) in Mu/Hu mice compared to those from Hu/Hu mice (Fig. 5G).

To assess the possible role of B cells in the development of autoimmunity in HIS mice, we treated Hu/Hu mice with rituximab (anti-CD20) once every 3 weeks from 20 to 38 weeks post-transplantation (Fig.6A). As shown in Fig. 6B, this treatment successfully depleted B cells from the circulation and eliminated serum IgM. Immunofluorescent analysis of serum IgM from rituximab treated mice showed an absence of autoreactive IgM (Fig. 6C). However, B cell depletion with this method did not prevent or even delay disease development (Fig. 6D), suggesting a minor, if any, role for antibodies in disease progression. However, since it remained possible that serum antibody was critical in presenting antigen to T cells and/or initiating inflammation that caused later disease, we also evaluated the impact of rituximab treatment early post-transplant. As shown in Fig. 6E, starting rituximab treatment one week post-transplant and continuing through the post-transplant course also failed to delay or reduce the development of disease and, surprisingly, significantly accelerated its development. From these results, we concluded that antibodies were not required for disease development.

Tfh- and Tph-like cells adoptively transfer disease in recipients containing human APCs without T cells: accelerated expansion and disease induction by T cells from Hu/Hu compared to Mu/Hu mice

To further clarify the role of Tfh- and Tph-like cells in the development of autoimmunity, we tested their ability to expand, differentiate, promote B cell differentiation and induce disease in a T cell adoptive transfer model. We first generated a cohort of Mu/Hu and Hu/Hu mice from the same human FL CD34 cell donor. Twenty-two weeks later, after T cells had reconstituted the spleen, we euthanized both groups of HIS mice and FACS sorted splenic $CD4^+CD45RA^-CD45RO^+PD\text{-}1^+CXCR5^+$ Tfh-like and $CD4^+CD45RA^-CD45RO^+PD\text{-}1^+CXCR5^-$ Tph-like cells. These T cells were adoptively transferred intravenously into thymectomized NSG mouse recipients that had received FL $CD34^+$ cells 12 weeks earlier from the same human donor. Since these latter recipients lacked an endogenous (murine) thymus and had not received a thymus graft, they reconstituted only with B cells and myeloid APCs derived from the fetal HSC donor and did not generate T cells, as we have previously reported[1,12] . Thus, there were 5 different recipient groups, (a) No T cell transfer (APC only, n = 3), (b) mice that received Tph-enriched (n = 5) or (c) Tfh-enriched cells (n = 3) from Hu/Hu mice, and mice that received (d) Tph-enriched (n = 5) and (e) Tfh-enriched cells (n = 3) from Mu/Hu mice (Fig. 7A). Fig. 7B illustrates the gating strategy used to isolate Tfh and Tph cells from donor spleens.

As shown in Fig. 7C-D, both Tfh-like and Tph-like cells originating in Hu/Hu mice expanded faster and to a greater extent than those originating in Mu/Hu mice, achieving higher circulating levels. Recipients of Tfh-like cells from Hu/Hu mice contained high numbers of circulating Tph-like and much lower numbers of Tfh-like cells (Fig. 7E, F), suggesting that Tfh-like cells might have lost CXCR5 expression or that Tph-like contaminants expanded preferentially. Recipients of Tph-like cells from Hu/Hu mice also contained low numbers of Tfh-like cells and much higher fractions of Tph-like cells, whose numbers and percentages were similar to those seen in recipients of Hu/Hu Tfh-like cells (Fig. 7F). Recipients of Mu/Hu Tfh-like or Tph-

like cells contained much lower numbers of human T cells of both types (Fig.7D-F), but T cells in the group receiving Mu/Hu Tfh-like cells also demonstrated a predominant Tph-like phenotype (Fig. 7F). Similar trends were seen in spleens at the time of sacrifice, though differences did not achieve statistical significance (Fig. S2, top row).

These differences in Tfh-like and Tph-like cell expansion from Hu/Hu vs Mu/Hu donor mice led us to compare B cell differentiation in the adoptive recipients. Proportions of B cells among human $CD45^+$ cells (Fig. 8A) reflected the degree of dilution due to expansion of transferred T cells noted above (Fig. 7D) and overall circulating B cell counts were similar between groups (Fig. 8A). No significant difference in proportions of naïve (IgD), memory (CD27) and IgG class-switched B cells was observed between the 4 groups and the APC-only HIS mouse control group, although there was a trend toward increased IgG^+ B cells in adoptive recipients of T cells at later time points (Fig. 8B).

By 5 weeks following adoptive transfer, the blood of recipients of Tfh and Tph cells from Hu/Hu mice exhibited increased levels of $CD11c^+$ B cells, an effector B cell population associated with aging, infection, and human autoimmune diseases, compared to recipients of T cells from Mu/Hu mice (Fig. 8C). This difference largely reflected an increase in the percentage of atypical B cells ($IgD^-CD27^-CD11c^+$, DN2) in the recipients of Hu/Hu T cells. Analysis of splenic B cell populations showed similar trends (Fig. S2). Both activated or age-associated B cells ($IgD^-CD27^+CD11c^+$) and atypical B cells ($IgD^-CD27^-CD11c^+$) were significantly increased in the spleens of recipients of Hu/Hu Tph and Tfh cells compared to recipients of Mu/Hu Tph and Tfh cells 9 weeks following adoptive transfer (Fig. 8C). Splenic total and naïve B cell percentages were not statistically different between groups (Fig.S2). However, spleens of recipients of Tfh-like and Tph-like cells from Hu/Hu mice contained higher percentages of memory B cells and of $CD11c^+$

B cells than those of Mu/Hu T cell recipients (Fig.S2, bottom row).

We also analyzed the levels of IgM and IgG from these 4 groups of recipient HIS mice and APC-only controls. Recipients of Tfh-like or Tph-like cells from Hu/Hu mice had higher levels of IgM and IgG antibodies compared to recipients of Tfh-like or Tph-like cells from Mu/Hu mice and the APC-only controls contained IgM at low levels and undetectable levels of IgG (Fig. 8D). Collectively, these results demonstrate a role for Tfh-like and Tph-like cells in inducing both IgM and IgG antibodies in HIS mice and show that T cells from Hu/Hu mice provide help for autologous B cell antibody responses more effectively than those from Mu/Hu mice.

Adoptive recipients of Tfh-like and Tph-like cells from Hu/Hu mice lost weight beginning at 7 and 9 weeks, respectively, whereas the recipients of Mu/Hu T cells did not show obvious weight loss (Fig. 8E). Clinical disease was also more apparent in recipients of Hu/Hu T cells, with the most rapid onset in recipients of Hu/Hu Tfh-like cells. In contrast, most recipients of Mu/Hu T cells did not develop clinically apparent disease during the follow-up period (Fig. 8F). Together, our data suggest that T cells developing in an autologous human thymus graft interact more effectively with peripheral B cells and other APCs, presumably reflecting thymic positive selection on the same HLA molecules as those in the peripheral APCs, resulting in T cell expansion, increased CD11c expression on B cells and eventually disease development.

Discussion

We recently demonstrated that human T cells play a requisite role in inducing a multi-organ autoimmune disease that develops in HIS mice that have a native murine or grafted human thymus and receive human $CD34^+$ cells intravenously. The disease is characterized by organ infiltration by human T cells and macrophages and develops more rapidly in mice with a native murine thymus (Mu/Hu mice), where they fail to undergo normal negative selection, apparently

due to the lack of a normal thymic structure, including a paucity of medullary epithelial cells[1]. In contrast, thymectomized HIS mice that receive human fetal thymus grafts (Hu/Hu mice) demonstrate negative selection for self antigens[1], have normal human cortico-medullary thymic structure and develop autoimmune disease significantly later[1]. The marked delay in disease development in Hu/Hu compared to Mu/Hu mice is mitigated by the presence of a murine thymus in non-thymectomized recipients of human thymus and $CD34^+$ cells[1], partially explaining the slower disease development in our model compared to studies in non-thymectomized "BLT" mice[19]. Another reason for the delay in disease development in our model is the measures taken to deplete thymocytes pre-existing in the thymus graft at the time of transplantation, as these also accelerate disease development[1]. Unlike GVHD induced by mature T cells transferred in human PBMCs[2], the slowly-evolving autoimmune disease (termed autoimmune because it is mediated by T cells developing *de novo* in the recipient rather than by cells carried in the graft) in our model is independent of direct recognition of murine antigens, as it develops with similar velocity in NSG mice that express MHC and in those that completely lack (due to β2m and CIITA knockout) murine Class I and Class II MHC antigens[1].

We have now demonstrated that autoimmunity in both Mu/Hu and Hu/Hu mice is associated with the appearance of Tph-like memory T cells and, to a greater extent in Mu/Hu than Hu/Hu mice, of Tfh-like cells in the circulation and spleen. Development of these T cell subsets is associated with differentiation of memory and class-switched B cells and characterized by the presence in serum of human IgM and IgG autoantibodies. The development of IgG autoantibodies was dependent on human T cells in HIS mice, consistent with previous literature[14-16]. While mice lacking T cells also generated low levels of IgM autoantibodies, IgM levels were markedly increased by the presence of T cells.

Importantly, our data indicate that neither B cells nor antibodies are required for disease development. All HIS mice in our studies contained IgM autoantibodies, regardless of the presence or absence of T cells, though total IgM levels were increased in the groups containing T cells. In mice, the majority of natural IgM autoantibodies are produced by splenic B1 cells. Many of these are polyreactive, demonstrate autoreactivity and may play a predominantly regulatory, protective role[20]. The high levels of IgM against specific antigens that were detected in sera of our HIS mice were consistent with polyreactivity, since the sum of their levels against 3 antigens was greater than total IgM levels in some cases. The lack of a functional C5 complement component, rendering membrane attack complex and C5a anaphylatoxin production impossible, may help to explain the lack of pathogenicity of autoantibodies observed in our studies and different results might be obtained in NSG recipients engineered to correct the C5 deficiency[21]. However, C3 and C4 cleavage products of more proximal complement component activation might be expected to mediate significant pathology[22] and we are therefore surprised that B cells did not play a more readily apparent role in driving disease. In fact, the acceleration of disease in animals depleted of B cells from the beginning of the post-transplant period suggests that B cells may play a predominantly regulatory role in this model. Nevertheless, it is noteworthy that adoptive recipients of Tph-like and Tfh-like cells from Hu/Hu mice demonstrated an increase (compared to counterparts receiving T cells from Mu/Hu mice) in CD11c^{+} B cells, an effector B cell population otherwise known as age-associated B cells that is increased in association with human autoimmune diseases[17,18]. These data directly demonstrate the capacity of Tfh- and Tph-like cells from Hu/Hu, and to a lesser extent, from Mu/Hu mice, to induce the differentiation of this unique B cell subset. Our adoptive transfer studies also directly demonstrate the capacity of Tfh- and Tph-like cells generated in HIS mice to induce class-switched IgG-expressing and IgG-secreting B cells.

In vitro studies demonstrated effective help for differentiation of autologous B cells by T cells that differentiate in an autologous human thymus graft and less effective T-B interactions for T cells that differentiated in the xenogeneic murine thymus. These results are consistent with the interpretation that positive selection in an autologous thymus generates T cells that interact more effectively with autologous human APCs and B cells than T cells generated in a murine thymus lacking HLA molecules. Indeed, T cells have been shown to be essential for B cell maturation in HIS mice[14] and increased IgG levels are detected in association with greater T cell reconstitution[14,23]. Furthermore, introduction of an HLA Class II molecule into the mouse has been reported to enhance human T-B cell interactions in HIS mice with a murine thymus[15,16].

In view of the improved T cell-B cell interactions in Hu/Hu compared to Mu/Hu mice, it is somewhat paradoxical that Mu/Hu mice demonstrate increased levels of class-switched IgG antibodies and increased activated/atypical B cells compared to Hu/Hu mice. However, we believe the failure to negatively select human autoreactive T cells in the murine thymus, as we have previously reported[1], may provide an explanation for this paradox. If human T cells developing in a murine thymus are not centrally tolerized to murine antigens presented by human APCs, they may be expected to react with human APCs loaded with murine antigens, including human B cells, in the periphery in a manner that resembles an alloresponse. Alloresponses can activate B cells and induce polyclonal class-switched antibody responses that include autoantibodies, as shown in MHC heterozygous (F1) mice receiving MHC homozygous parental T cells, eliciting a GVH response that manifests as autoimmunity with autoantibodies, referred to as "lupus-like" GVHD[24,25]. Consistent with this possibility, responses of Mu/Hu splenic CD4 T cells to mouse antigen-loaded human dendritic cells were stronger than those of Hu/Hu splenic T cells. Additionally, the increase in activated/age-associated ($IgD^{-}CD27^{+}CD11c^{+}$) and atypical (IgD^{-}

CD27$^-$CD11c$^+$) B cells in Mu/Hu compared to Hu/Hu mice points to increased B cell activation in Mu/Hu mice.

The observed absence of a role for B cells in disease development thus requires alternative explanations for the more rapid disease development in Mu/Hu than Hu/Hu mice. Additional studies indicate that LIP of T cells entering the periphery is increased in Mu/Hu compared to Hu/Hu mice, in which thymopoiesis and peripheral T cell reconstitution is more robust, and that LIP plays a significant role in the development of disease (M. Khosravi-Maharlooei et al, manuscript in preparation). Consistently, studies in mice have strongly implicated LIP in autoimmune disease development[26-29].

The adoptive transfer studies described here, in which Tfh- and Tph-like cells from Hu/Hu mice induced more rapid disease than those from Mu/Hu mice, demonstrated the relative disease-causing potential of these cells in the absence of variations in T cell reconstitution, as the cells were introduced to identical, completely T cell-deficient environments. Adoptive transfer of Hu/Hu T cells led to more rapid expansion than that of Mu/Hu T cells, suggesting that recognition of the same HLA antigens in the periphery as those mediating thymic positive selection optimizes LIP. This increased LIP may account for the more rapid disease development in the recipients of Hu/Hu than Mu/Hu Tfh- and Tph-like cells. Consistent with this interpretation, we have previously demonstrated that human peripheral APCs are absolutely required for survival, LIP and effector differentiation of Hu/Hu T cells[30]. As reported for murine T cells[31,32], rapid LIP of human T cells is likely to be antigen-driven. Given that indirect presentation of murine antigens on human APCs is sufficient to drive disease[1] and is required for survival of transferred human T cells[30], we conclude that incomplete negative selection of indirectly xenoreactive mouse-specific T cells (possibly recognizing tissue-restricted antigens normally produced by murine thymic epithelial

cells, which are absent in human thymus grafts) in a human thymus allows these T cells to recognize murine peptides presented on human APCs. This interpretation is consistent with our findings *in vitro* of tolerance to murine antigens presented directly on murine DCs, since murine APCs are present in the human thymic medulla of Hu/Hu mice[3] and of weak but measurable reactivity to autologous DCs capable of presenting murine antigens indirectly.

While lack of tolerance to murine antigens in the primary Mu/Hu mice reflects the lack of medullary structure and of central tolerance in the native mouse thymus[1], the number of these T cells that expand in the periphery may be constrained by their positive selection on murine cortical epithelium and MHC, resulting in a more oligoclonal (compared to Hu/Hu mice) expansion of T cells recognizing murine peptides presented on human APCs expressing HLA. This situation is exacerbated by the markedly reduced diversity of the human TCR repertoire selected in the native murine thymus vs the human thymus graft[1]. The extensive expansion of a smaller population of peripheral T cells in Mu/Hu compared to Hu/Hu mice may have resulted in exhaustion of Tfh- and Tph-like cells in Mu/Hu mice prior to the time of transfer, delaying disease onset in adoptive recipients. Exhaustion has been reported for human T cells in HIS mice with GVHD[33] and chronic HIV infection[23]. The observed inability of direct antigen presentation on murine cells to drive LIP[30] or disease development[1], and hence dependence on antigen presentation on human APCs likely reflects failed coreceptor, costimulatory, adhesive and/or cytokine interactions between human T cells and murine cells. While this *in vivo* result may seem inconsistent with the increased reactivity to murine antigens *in vitro* of T cells from Mu/Hu compared to those from Hu/Hu mice, human APCs were also present in these cultures, resulting in an inability to specifically assess direct xenoreactivity.

An additional possible contributor to accelerated autoimmune disease development in

Mu/Hu compared to Hu/Hu mice may be inferior Treg function in the Mu/Hu group due to the incompatibility of the MHC of the murine thymic epithelium and the paucity of medullary epithelium responsible for positive selection of Tregs, resulting in a deficiency of Tregs that are capable of interacting with human APCs in the periphery or capable of recognizing murine antigens directly. This interpretation is consistent with the known role of Tregs in regulating Tfh activity[34].

Tfh and Tph are subsets of human effector T cells that are closely related and have been implicated in autoimmune diseases, yet have distinct phenotypes and functions, with Tfh providing help for naïve B cell differentiation and Tph acting predominantly on memory B cells[35]. Tfh are found largely in lymphoid tissues while Tph are generally found in inflamed tissues, though both seem to have a circulating component. Ratios of Bcl-6 to Blimp1 transcription factors are lower for Tph than Tfh and Tph have been suggested to drive extrafollicular differentiation of age-related B cells in autoimmune disease[35,36]. While it is unknown whether there is plasticity/interchangeability between these subsets, our adoptive transfer studies are the first, to our knowledge, to suggest that there may be. In these studies, Tph-enriched T cells showed greater proliferative capacity overall than Tfh-enriched populations from Hu/Hu and Mu/Hu mice. Remarkably, the final number of Tph-like cells was quite similar and more than an order of magnitude higher than that of Tfh in recipients of either Tfh or Tph-enriched populations, suggesting that Tfh may have the capacity to transition to the Tph phenotype when they expand in a lymphopenic environment. However, we cannot rule out the expansion of a contaminating Tph population in the sorted Tfh preparations, and fate-mapping studies will be needed to definitively address this question.

In summary, our data directly demonstrate the pathogenicity and capacity to induce

antibody secretion of expanded human Tph- and Tfh-like cells and implicate both limitations in thymic selection and LIP as factors driving the development of autoimmune disease in human immune system mice. Since Tfh, Tph, autoantibodies and LIP have all been implicated in various forms of human autoimmune disease, the observations here provide a platform for the further dissection of human autoimmune disease mechanisms and therapies.

Acknowledgements: We thank Dr. Remi Creusot for critical reading of the manuscript and Ms. Julissa Cabrera for assistance in its preparation. We also thank Dr. Emmanuel Zorn for providing control supernatants of cell lines expressing cloned polyreactive B cell receptors. This work was supported by NIH grants #P01 AI 045897 and U01 DK 123559.

FIGURE LEGENDS

Figure 1. Lack of tolerance to murine recipient antigens of CD4 T cells developing in mouse thymus compared to those developing in human thymus. Mu/Hu (n=4) and Hu/Hu (n=4) mice were sacrificed 20 weeks after transplantation and their splenocytes were CFSE-labeled and tested for reactivity to various antigen-presenting cells. To test direct reactivity to autologous human DCs, FL $CD34^+$ cells used to generate both Hu/Hu and Mu/Hu mice were differentiated into dendritic cells. NSG DCs were generated from bone marrow progenitors. Proliferation of T cells was measured after 6 days of coculture based on CFSE dilution. (A) Representative plots showing proliferation of HuHu (top) and MuHu (bottom) T cells following co-culture with autologous human DCs, NSG mouse DCs, autologous human DCs loaded with murine antigens or with no DC. (B) Frequencies of proliferating $CD3^+$ T cells and $CD4^+$ and $CD8^+$ T cells from splenocytes of HuHu (red) and MuHu (blue) mice in response to the indicated DCs. Differences between

proliferation rate of Hu/Hu and Mu/Hu T cells were analyzed with unpaired t test. In all graphs, each point represents an individual mouse with the mean indicated by a black line. Asterisks indicate statistical significance. ** $P < 0.01$, * $P< 0.05$ comparing Mu/Hu and Hu/Hu groups. Statistically significant differences in responses between Hu/Hu or Mu/Hu T cells compared to the same group of T cells stimulated with other DCs are indicated by red and blue asterisks, respectively, while differences between Hu/Hu and Mu/Hu T cells are marked with black asterisks.

Figure 2. Tfh and Tph cell reconstitution in HIS mice. (A) Schematic of experimental design; (B) Representative staining; (C,D) percentage of CXCR5-PD-1$^+$ Tph and CXCR5$^+$PD-1$^+$ Tfh cells among CD4$^+$CD45RA$^-$ T cells and absolute counts per microliter in peripheral blood of HIS mice with mouse thymus (*n = 19*) or human thymus (*n = 29*) from week 12 to week 32 post-transplantation, analyzed every two weeks; (E) Representative staining and (F,G) percentage of CXCR5$^-$PD-1$^+$ Tph and CXCR5$^+$PD-1$^+$ Tfh cells among CD4 T cells and absolute counts in spleens of HIS mice with mouse thymus or human thymus at <20W, 20-30W and >30W post-transplantation. (H) Expression of ICOS in Tph and Tfh from Mu/Hu (n=16) and Hu/Hu (n=8). Mice (combined results) and (I) IL-21 cytokine production after PMA/ionomycin stimulation of Tph (CXCR5$^-$PD- 1$^+$) and Tfh cells (CXCR5$^+$PD-1$^+$) compared to naive CD4$^+$ T cells (grey) from Mu/Hu (n=11) and Hu/Hu (n=4) mice (combined results). The results are expressed as mean ± SEM geometric mean fluorescence intensity (MFI) values; (J,K) percentage of ICOS$^+$ and FOXP3$^+$cells among splenic Hu/Hu and Mu/Hu Tfh and Tph cells. All data are shown as means ± SEM. Asterisks indicate statistical significance between Hu/Hu and Mu/Hu groups as calculated by Bonferroni multiple comparison test *$p< 0.05$,

**$p< 0.01$, ***$p< 0.001$ and ****$p< 0.0001$.

Figure 3. IgG and IgM antibodies, Tfh and Tph cell phenotypes and B helper function of T cells from Mu/Hu vs Hu/Hu mice. (A) Absolute concentrations of $CD19^+$ B cells in peripheral blood of HIS mice with mouse thymus (*n = 19*) or human thymus (*n = 29*) from week 12 to week 32 post-transplantation, analyzed every two weeks; and their (B) plasma IgM and IgG concentrations; (C) FACS-sorted Tfh ($CD4^+CD19^-CD45RA^-CXCR5^+CD25^-$) and Tph ($CD4^+CD19^-CD45RA^-CXCR5^-CD25^-$) cells from spleens of HIS mice with mouse vs human thymus were co-cultured with naïve B cells ($CD4^-CD19^+CD38^-IgD^+CD27^-$) and SEB as described in Materials and Methods and plasmablast differentiation was assessed. (D) Percentage of naïve splenic B cells that differentiated into plasmablasts ($CD4^-CD19^+CD20^-CD38^+$) following co-culture with Tfh or Tph cells from HIS mice with mouse thymus (*n = 11*) or human thymus (*n = 12*) sacrificed at <20 weeks or >20 weeks post-transplantation. Splenocytes were obtained in the indicated time ranges. (E) Concentration of CXCL13 chemokine from plasma of HIS mice with mouse thymus (*n = 12*) or human thymus (*n = 13*). For (A-B-G), Bonferroni multiple comparison test was used. For (C-D) Friedman test was performed and corrected using Dunn's multiple comparisons test. For (F), Wilcoxon matched pairs signed rank test was used. Data are represented as mean ± SEM. *p< 0.05, **p< 0.01, and ****p< 0.0001.

Figure 4. B cell follicles in HIS mice. (A) H&E staining and immunofluorescence performed for CD20, CD3, and PNA in serial tissue sections of spleen from HIS mice with mouse vs human thymus at <20W, 20-30W and >30W post transplantation. Confocal imagines (10x) showing follicles ($CD20^+$) and T cell zones ($CD20^-$). (B) Quantification of follicular area in pixels between HIS mice with mouse vs human thymus. (C) Quantification of the numbers of follicles and follicular area in pixels over time, combining both groups of mice. Asterisks indicate statistical significance as calculated by Kruskal-Wallis. *p< 0.05, and ***p< 0.001. White squares in the H&E

images indicate the area represented on the right side. White bar = 100µm. An average of three different slides was examined per sample.

Figure 5. IgM and IgG antibodies from HIS mice are self-reactive. (A) NSG intestine stained with serum from HIS mice with mouse or human thymus or with naïve NSG mouse serum and secondary antibodies against human IgM and IgG. DAPI was used for nucleic acid staining. (B-C) Total concentration of serum IgM antibody and concentration of IgM antibody reactive to LPS, insulin and dsDNA. (D) total concentration of serum IgG antibody; (E) concentrations of IgG antibody reactive to LPS, insulin and dsDNA. RU were defined as relative units compared to control supernatants from monoclonal polyreactive IgG-producing cell cultures. (F) Percentage of total serum IgM antibody that was reactive to LPS, insulin and dsDNA from total IgM of HIS mice with mouse (n = 11) vs human thymus (n = 15) at <20W, 20-30W and 30W post-transplantation. (G) Percentage of $CD11c^+$ $CD27^+$ and $CD11c^+$ $CD27^+$ in IgG^- $CD19^+$ B cells in the spleens of donor Hu/Hu and Mu/Hu mice. Asterisks indicate statistical significance as calculated by t-test *$p < 0.05$.

Figure 6. B cell depletion does not prevent disease development. (A) HIS mice with mouse thymus were generated as described in Materials and Methods and were injected intraperitoneally with 1mg of rituximab (anti-CD20) or PBS every 3 weeks from W20 to W38. (B) Frequency and absolute number of $CD19^+$ B cells and serum IgM concentration before (grey) and after (white) treatment in HIS mice treated with rituximab or PBS (control). (C) NSG tissue stained with (primary) serum from HIS mice with mouse thymus and secondary antibodies against human IgM. DAPI was used for nucleic acid staining. (D) Kaplan-Meier curves for disease-free survival in

relation to rituximab treatment in HIS mice with mouse thymus (n=6 per group). (E) Schema for early rituximab treatment initiation, Kaplan-Meier curves showing disease-free survival of each group and serum IgM levels in rituximab-treated and PBS-treated control group (n=6 per group). All data are shown as means ± SEM. Asterisks indicate statistical significance as calculated by Bonferroni multiple comparison test **p< 0.01 and ****p< 0.0001.

Figure 7. Expansion of donor T cells in thymecomized recipient HIS mice. (A) Schema for adoptive transfer experiment. Purified Tph or Tfh cells from reconstituted mice with mouse vs human thymus were adoptively transferred to thymectomized NSG mice that had received HSCs 12 weeks earlier from the same fetal liver $CD34^+$ cell donor but did not receive a thymus graft. These mice therefore had B cells and other APCs but not T cells at the time of adoptive transfer. (B) The gating strategy used to isolate Tfh and Tph cells from donor spleens. (C) Representative plot of $CD3^+$ T cells and $CD19^+$ B cells in APC-only mice (*n = 3*), adoptive recipients of Tph cells (*n = 5*) or Tfh cells (*n = 3*) from HIS mice with human thymus (Hu/Hu), or adoptive recipients of Tph cells (*n = 5*) or Tfh cells (*n = 3*) from HIS mice with mouse thymus (Mu/Hu). (D) Frequency and absolute number of $CD3^+$ T cells. (E-F) Frequencies and absolute numbers of $CXCR5^+PD\text{-}1^+$ Tfh and $CXCR5^-PD\text{-}1^-$ Tph cells, respectively, in indicated groups. Asterisks indicate statistical significance as calculated by Bonferroni multiple comparison test *p<0.05, **p<0.01, ***p<0.001 and ****p<0.0001. The green asterisks show significant differences between the Tph in Hu/Hu vs Mu/Hu mice, while the orange asterisks show significant differences between the Tfh in Hu/Hu vs Mu/Hu mice.

Figure 8. Effects of transferring Tfh and Tph from Mu/Hu and Hu/Hu mice to recipient HIS mice containing human APCs but not T cells. (A) Frequencies and absolute numbers of B cells, (B) percentages of IgD^+CD27^-, IgD^+CD27^+, IgD-CD27+, IgD^-CD27^-, IgM^+IgD^+ and IgG^+ B cells among $CD19^+$ B cells, (C) Percentages of $CD11c^+$ B cells among $CD19^+$ B cells in the blood of APC-only mice (n = 3), recipients of Tph cells (n = 5) or Tfh cells (n = 3) from HIS mice with human thymus (Hu/Hu), and recipients of Tph cells (n = 5) or Tfh cells (n = 3) from HIS mice with mouse thymus (Mu/Hu). Percentage of $CD11c^+$ $CD27^+$ and $CD11c^+$ $CD27^-$ in IgD^- $CD19^+$ B cells in the spleen and blood (W9 of adoptive transfer) of adoptive recipient mice. (D) IgM (left) and IgG (right) concentrations in sera of recipient mice before and after adoptive transfer. (E) Average weights over 16 weeks following adoptive transfer. (F) Kaplan-Meier curves for disease-free survival following injection of Hu/Hu Tph or Tfh or Mu/Hu Tph or Tfh cells. Animals were scored for autoimmune disease appearance every 2 weeks using a modification of published GVHD scales[37,38] and considered to have disease if their score was >3 or if they showed >20% weight loss. Asterisks indicate statistical significance as calculated by Bonferroni multiple comparison test between Hu/Hu Tph and Mu/Hu Tph, or Hu/Hu Tfh and Mu/Hu Tfh cells. *$p<0.05$, **$p<0.01$ and ***$p<0.001$. Mantel-Cox test was used to analyze statistical significance in survival curve experiment.

Table 1. Mouse tissue-reactive human IgM and IGG in serum of Mu/Hu and Hu/Hu mice.

			Pancreas	Liver	Spleen	Kidney	Thymus	SI	SG	Skin	AG	LI	Bone	Lung
Control Mouse	NSG	IgM	-	-	-	-	-	-	-	-	-	-	-	-
		IgG	-	-	-	-	-	-	-	-	-	-	-	-
Humanized, no thymus <20W	mouse #1	IgM	+	+	+	+	+	+	+	+	+	+	+	+
		IgG	-	-	-	-	-	-	-	-	-	-	-	-
	mouse #2	IgM	+	+	+	+	+	+	+	+	+	+	+	+
		IgG	-	-	-	-	-	-	-	-	-	-	-	-
Mouse Thymus <20W	mouse #3	IgM	+	+	+	+	+	+	+	+	+	+	+	+
		IgG	-	-	-	-	-	-	-	-	-	-	-	-
	mouse #4	IgM	+	+	+	+	+	+	+	+	+	+	+	+
		IgG	-	-	-	-	-	-	-	-	-	-	-	-
	mouse #5	IgM	+	+	+	+	+	+	+	+	+	+	+	+
		IgG	+	+	+	+	+	+	+	+	+	+	+	+
Mouse Thymus >30W	mouse #6	IgM	+	+	+	+	+	+	+	+	+	+	+	+
		IgG	+	-	-	+	+	+	-	+	-	+	+	+
	mouse #7	IgM	+	+	+	+	+	+	+	+	+	+	+	+
		IgG	-	-	-	-	-	-	-	-	-	-	-	-
	mouse #8	IgM	+	+	+	+	+	+	+	+	+	+	+	+
		IgG	-	-	-	-	-	-	-	-	-	-	-	-
Human Thymus >30W	mouse #9	IgM	+	+	+	+	+	+	+	+	+	+	+	+
		IgG	-	-	-	-	-	-	-	-	-	-	+	-
	mouse #10	IgM	+	+	+	+	+	+	+	+	+	+	+	+
		IgG	-	-	-	-	-	-	-	-	-	-	-	-
	mouse #11	IgM	+	+	+	+	+	+	+	+	+	+	+	+
		IgG	-	-	-	-	-	-	-	-	-	-	-	-

SI, small intestine; SG, salivary gland; AG, adrenal gland; LI, large intestine

Table 2: GVHD scoring system to assess disease severity based on five parameters: weight loss, posture, activity, fur condition, and skin condition.

Parameter	Criteria	Score
Weight Loss	10–25% weight loss compared to baseline	1
	>25% weight loss compared to baseline	2
Posture	Slight kyphosis	0.5
	Obvious kyphosis	1
	Kyphosis	1.5
	Severe kyphosis	2
Activity	Decreased activity	0.5
	Stationary >50% of the time	1
	Moves when stimulated	1.5
	No movement	2
Fur Condition	Ventral ruffling	0.5
	Ventral line and slight back ruffling	1
	Ruffling >50% of the body	1.5
	Ruffling entire body and denuded skin	2
	Flaking of ears, tail, or paws	0.5

Skin Condition	Erythema in tail or anus, ear shriveling	1
	Open lesions	1.5
	Multiple open lesions	2

Materials and Methods

Animals and tissues

NSG (NOD.Cg-*Prkdc*^{scid} *Il2rg*^{tm1Wjl}) mice were purchased from Jackson Laboratory (Bar Harbor, ME) and were housed and bred in specific pathogen-free helicobacter and Pasteurella pneumotropica-free conditions in the Animal Facility at Columbia University Medical Center. Human fetal thymus and fetal liver (FL) tissues (gestational age 17 to 20 weeks) were obtained from Advanced Biosciences Resources. Fetal thymus fragments were cryopreserved in 10% dimethyl sulfoxide (Sigma-Aldrich) and 90% human AB serum (Gemini Bio Products). FL fragments were treated for 20 minutes at 37°C with 100 µg/mL of Liberase (Roche) to obtain a cell suspension. Human CD34^{+} cells were isolated from FL by density gradient centrifugation (Histopaque-1077, Sigma) followed by positive immunomagnetic selection using anti-human CD34 microbeads (Miltenyi Biotec) according to the manufacturer's instructions. Cells were then cryopreserved in liquid nitrogen. Studies were approved by the Animal Care and Use Committee at Columbia University. All human samples were collected with approval of the Institutional Review Board of Columbia University Medical Center in accordance with the Declaration of Helsinki.

Clinical definition of autoimmune disease

The definition of autoimmune-like disease after humanization with HSCs or following adoptive T cell transfer to T cell-deficient HIS mice is based on a GVHD scoring system described in our

earlier publication[1]. This system evaluates five criteria: percentage of weight loss, posture, activity level, fur condition, and skin condition, with each parameter assigned a grade from 0 to 2 (Table 2). For the disease-free survival curve (Fig. 6 and 8F), a total score exceeding 3 or >20% weight loss was classified as indicative of disease.

Human fetal tissue transplantation

To generate HIS mice with human thymus (Hu/Hu mice), 6-8-week old NSG mice were thymectomized and allowed to recover for two weeks, then sublethally irradiated (1.0-1.2 Gy) using an RS-2000 X ray irradiator (Rad Source Technologies, Inc., Suwanee, GA). Human fetal thymus fragments of about 1 mm^3 were implanted beneath the kidney capsule and 2×10^5 human FL $CD34^+$ cells were injected IV. Recipient mice received intraperitoneal injections of 400 µg of anti-human CD2 monoclonal antibody BTI-322 or Lo-CD2 26 (Bio X Cell, Inc) on days 0, 7, and 14 post-transplantation. HIS mice with intact mouse thymus (Mu/Hu mice) were generated simultaneously and received similar treatment without thymus transplantation.

Flow Cytometry

Human reconstitution, Tfh cells, Tph cells and B cells were monitored in PBMC from 8 weeks after transplantation and in spleens of HIS mice until endpoint. Single-cell splenocyte suspensions and blood samples were treated with ACK lysis buffer (Life Technologies) to remove erythrocytes. After ACK erythrocyte lysis, remaining spleen cells were passed through a 70µm filter prior to staining for FCM analysis. All cells were stained for detection of surface ICOS (ISA-3), CD45RA (HI100), CCR7 (G043H7), PD-1 (EH12.2H7), CXCR5 (RF8B2), CD8 (RPA-T8), CD25 (2A3),

CD3 (SK7), CD4 (RPA-T4), CXCR3 (1C6), CD127 (A019D5), CCR2 (1D9), CCR5 (2D7), CD20 (L27), CD19 (HIB19), IgM (G20-127), IgG (G18-145), IgA (IS11-8E10), IgD (IA6-2), CD27 (O323), CD38 (HIT2), CD138 (MI15), CD11c (B-ly6), CD14 (M5E2), CD21 (Bu32), hCD45 (HI30) and mCD45 (30-F11). To detect IL-21, cells were stimulated for 3 hours with 50 ng/ml phorbol myristic acid (PMA; Sigma-Aldrich, St Louis, MO, USA), 1 μg/ml ionomycin (Sigma-Aldrich) and 3 μg/ml brefeldin A in RPMI supplemented with 10% FBS, 1% Hepes (Sigma-Aldrich), 1% penicillin-streptomycin (Life Technologies), and 0.05% gentamicin (Life Technologies) in 37°C, 5% CO2 incubator conditions. For intracellular staining, single-cell suspensions were fixed-permeabilized with the FOXP3 Fixation Kit (Invitrogen) for 45 minutes at RT and then stained with mAbs for IL-21 (3A3-N2.1) for 30 minutes at RT in permeabilization buffer. After washing, cells were acquired on Aurora Cytek (Fremont, California) and on FACS FORTESSA (BD Biosciences), and analyzed with FlowJo v10 (Tree Star, USA) software.

Proliferative responses of HIS mouse T cells to human and mouse antigens.

Mu/Hu and Hu/Hu mice were sacrificed 20 weeks after transplantation and their splenocytes (not purified, so multiple murine and human cell populations were present) were CFSE-labeled and tested for reactivity to various antigen-presenting cells. To test direct reactivity to autologous human DCs, FL $CD34^+$ cells used to generate both Hu/Hu and Mu/Hu mice were differentiated into dendritic cells. Briefly, HSCs were cultured in Aim-V medium containing 10% human serum and stem cell factor (SCF, 50ng/ml) and granulocyte-macrophage colony-stimulating factor (GM-CSF, 50ng/ml) for 3 days. After 3 days, additional GM-CSF (100ng/ml) and SCF (50ng/ml) and low dose TNF-α (1ng/ml) were added to the culture. At day 7, cells were washed and cultured in medium containing GM-CSF (100ng/ml), IL-4 (20ng/ml) and TNF-α (2ng/ml). One week later,

differentiated DCs were harvested and either activated with prostaglandin E2 (PG-E2, 3000ng/ml) and TNF-α (20ng/ml) or incubated with apoptotic (irradiated at 30Gy) NSG mouse DCs for 12h for indirect presentation of mouse antigens, followed by activation with PG-E2 and TNF-α. To generate NSG mouse DCs, mouse bone marrow cells were cultured in AIM-V media containing 10% FBS and murine IL-4 (5 µg/ml) and GM-CSF (3 µg/ml). After 1 week, mouse DCs were harvested and either activated with LPS (1µg/ml) for 8h for direct presentation or irradiated (30Gy) for coculture with human DCs (for indirect presentation of mouse antigens on human DCs).

Splenocytes from Hu/Hu and Mu/Hu mice were stained with CFSE and cultured with various DCs (Auto human DCs, NSG DCs, Auto DCs loaded with mouse antigens, or no DCs) at a 10:1 ratio of splenocytes:DCs (100K CFSE-stained splenocytes and 10K DCs) in U-bottom 96-well plates. After 6 days, cells were stained with antibodies against human CD3, CD4 and CD8 and analyzed with a flow cytometer.

T-B-cell interaction assay

Single-cell splenocyte suspensions were stained with a panel to detect CD4 (RPA-T4), CXCR5 (RF8B2), CD45RA (HI100), CD19 (HIB19), IgD (IA6-2), CD27 (O323) and CD38 (HIT2) and prepared for sorting on BD FACSAria Fusion II. Cells were fist gated based on single cells and lymphocytes, and then Tfh cells ($CD4^+CD45RA^-CXCR5^+CD25^-$), Tph cells ($CD4^+CD45RA^-CXCR5^-CD25^-$) and naive B cells ($CD19^+CD38^-CD27^-IgD^+$) were FACS sorted. Cells were collected in RPMI 1640 (Life Technologies) supplemented with 10% FBS (Life Technologies). After collection, 20 x 10^3 Tfh cells or Tph cells and naïve B cells ($CD19^+CD38^-CD27^-IgD^+$) were incubated in the presence of staphylococcal enterotoxin B (SEB) (0.1 µg/ml) in a 1:1 ratio (T cells:B cells). Cultures were performed in V-shaped 96-well plates in RPMI 1640 (Life

Technologies) supplemented with 10% FBS, 1% Hepes (Sigma-Aldrich), 1% penicillin-streptomycin (Life Technologies), and 0.05% gentamicin (Life Technologies) in 37°C, 5% CO_2 incubator conditions. After 7 days, cell pellets were harvested and stained to analyze plasmablast differentiation ($CD19^+CD20^-CD38^+$).

Plasma CXCL13 levels

Whole peripheral blood (in heparin) was centrifuged at 1000 rpm for 15 minutes to collect plasma. Plasma was further centrifuged at 13000 rpm for 10 minutes to remove debris. CXCL13 was evaluated in EDTA plasma by ELISA assay (Human CXCL13/BLC/BCA-1 Quantikine® ELISA Kit, R & D Systems) following the manufacturer's instructions.

Plasma IgM and IgG levels

To quantify human antibodies in sera of HIS mice, diluted samples were added to plates(Corning Inc., Corning, NY) coated with goat anti-human IgG Fcγ fragment (Jackson) or goat anti-human IgM (Southern Biotech) overnight at 4°C. Plates were then washed in PBS with 0.05% Tween 20, and blocked with 2% Bovine Serum Albumin (BSA, Fisher Scientific). Bound human Ig was detected using biotin-conjugated mouse anti-human IgG (BD Pharmingen) or biotin-conjugated mouse anti-human IgM (BD Pharmingen) secondary antibodies, followed by streptavidin-horseradish peroxidase (Thermo Scientific). Colorimetric change by 3,3′,5,5′-Tetramethylbenzidine substrate solution (Thermo Scientific) was stopped by 2M sulfuric acid (Sigma), and optical densities determined by spectrophotometer absorbance at 450nm. Human serum with known IgM and IgG concentrations (Bethyl) was used to establish standard curves.

Assessment of reactivity to Insulin, dsDNA, LPS molecules

To determine the reactivity of serum antibodies to insulin, dsDNA, and LPS, polystyrene plates (Corning) were coated overnight at 4°C with 10 µg/mL LPS, 10 µg/mL dsDNA or 10 µg/mL recombinant human insulin (Sigma Aldrich, St. Louis, MO). After five washes in PBS with 0.05% Tween 20, serum was added and incubated for 2h at room temperature. Plates were then washed in PBS with 0.05% Tween 20, incubated for 1h with either horseradish peroxidase (HRP)-conjugated goat anti-human IgM or IgG (Invitrogen, Camarillo, CA), washed again, and developed using 3, 3', 5, 5'-tetramethylbenzidine (eBioscience, San Diego, CA). Optical density was read at 450 nm absorbance. Supernatants from polyreactive IgM and IgG B cell cultures generated as described[39] and provided by Dr. Emmanuel Zorn (Columbia University) were used to establish standard curves.

Histopathological analysis for HIS mouse models

For post-mortem histopathology, spleen from HIS mice were excised, fixed in zinc-formalin (Sigma) and embedded in paraffin. Serial 5-µm sections were stained with hematoxylin and eosin (H&E) and images were acquired using Aperio AT2 (Leica Biosystems, Wetzlar, Germany).

Immunofluorescence

Spleens from HIS mice were fixed with formalin and embedded in paraffin. FFPE tissues were cut using a Leica microtome at 5 µm. Cuts were done sequentially, placed on slides and left to dry for

24 hours prior to antibody staining. Tissues were deparaffinized and rehydrated by warming at 60°C for 1 hour followed by a serial bath of xylene and ethanol dilutions (100%, 95%, 80%, 70%, water). Antigen retrieval was performed using Borg RTU de-cloaking solution and a pressure cooker. The pressure cooker was set for 15 minutes at 11°C. Antigen retrieval was followed by permeabilization with confocal buffer for 1 hour. Titrated primary antibodies were added and left at 40°C overnight. Tissues were washed 3 times in 1x PBS and blocked with mouse and/or goat serum for 1 hour. Then anti-human CD3 Alexa Fluor 488 (UCHT1, Biolegend, 1:50 dilution), anti-human CD20 Alexa 647 (Abcam, EPR1622Y) and peanut agglutinin (PNA/germinal center) antibodies were incubated for 1 hour at room temperature followed by 3 washes, then incubation with secondary antibodies for 2 hours. Tissues were washed again in 1x PBS followed by staining with nuclear marker DAPI and Fluoromount G mounting media.

For detection of mouse-reactive human IgM and IgG antibodies, sera from HIS mice were incubated on pancreas, liver, spleen, kidney, thymus, small intestine, large intestine, skin, bone, and lung sections taken from a naïve NSG mouse. After incubation for 2 hours at room temperature, serum was washed away and secondary anti-human IgM and IgG antibodies were added for detection for 2 hours at room temperature. Negative controls were incubated with either no serum or naïve NSG mouse serum followed by secondary antibodies.

B cell depletion experiments

A group of Mu/Hu mice were generated (Fig. 6A) with irradiation (1Gy) followed by injection with fetal liver $CD34^+$ HSCs. Starting at week 20 post-transplantation, mice were injected with rituximab (1mg diluted in 1ml of PBS, injected intraperitoneally) every 3 weeks until week 38. Blood was drawn at various time points before and after rituximab injection to measure human

immune cell reconstitution in the blood and IgM levels in the serum. Mice were followed and evaluated for development of autoimmunity.

In another experiment (Fig 6E), Hu/Hu mice generated as described above received intraperitoneal injections of rituximab (1mg/mouse/injection) starting from week 1 and every 3 weeks until week 31, mice were. Serum IgM was checked with ELISA and mice were followed and evaluated for the development of autoimmunity.

Adoptive transfer experiment

Donor Mu/Hu and Hu/Hu mice were sacrificed at 22 weeks and $CD4^{+}CD45RA^{-}CD45RO^{+}PD\text{-}1^{+}CXCR5^{+}$ Tfh and $CD4^{+}CD45RA^{-}CD45RO^{+}PD\text{-}1^{+}CXCR5^{-}$ Tph cells were FACS sorted from their pooled (for each donor type) splenocyte suspensions. 2.5 x 10^{5} Tfh cells or Tph cells were adoptively transferred intravenously into recipient mice. The recipients were thymectomized NSG mice reconstituted 12 weeks earlier with the same HSCs as the Tfh/Tph donors, without athymus transplant, which therefore contained autologous human APCs but no T cells. Adoptive recipient mice were monitored for disease and peripheral blood was collected from the tail vein once a week. After 9 weeks, adoptive recipient mice were euthanized. Spleens and blood were collected and stained for Tfh, Tph and B cell analysis. Plasma was also collected for IgM and IgG evaluation.

Statistical methods

Statistical analyses and comparisons were performed with Graph-Pad Prism 8.0 (GraphPad Software). All data are expressed as average ± standard error of mean. The nonparametric Mann-Whitney U test was used to compare two groups. One-way analysis of variance (ANOVA) with

post-hoc Tukey test was performed to compare three groups. Two-way ANOVA was used to resolve overall effects between transplant groups over time. When two-way ANOVA was significant, Bonferroni's multiple comparison test was run. Spearman's correlation coefficient was computed to study the strength of correlation between quantitative variables. Wilcoxon matched pairs signed rank test was used when analyzing paired groups. Mantel-Cox tests were used to measure significance of differences in Kaplan-Meier survival curves. $P < .05$ was considered to be statistically significant.

References.

1 Khosravi-Maharlooei, M. *et al.* Role of the thymus in spontaneous development of a multi-organ autoimmune disease in human immune system mice. *Journal of autoimmunity* **119**, 102612 (2021).

2 Brehm, M. A. *et al.* Lack of acute xenogeneic graft- versus-host disease, but retention of T-cell function following engraftment of human peripheral blood mononuclear cells in NSG mice deficient in MHC class I and II expression. *FASEB J* **33**, 3137-3151 (2019).

3 Kalscheuer, H. *et al.* A model for personalized in vivo analysis of human immune responsiveness. *Science translational medicine* **4**, 125ra130 (2012).

4 Lan, P. *et al.* Induction of human T cell tolerance to porcine xenoantigens through mixed hematopoietic chimerism. *Blood* **103**, 3964-3969 (2004).

5 Lan, P., Tonomura, N., Shimizu, A., Wang, S. & Yang, Y. G. Reconstitution of a functional human immune system in immunodeficient mice through combined human fetal thymus/liver and CD34+ cell transplantation. *Blood* **108**, 487-492 (2006).

6 Melkus, M. W. *et al.* Humanized mice mount specific adaptive and innate immune responses to EBV and TSST-1. *Nature medicine* **12**, 1316-1322 (2006).

7 Khosravi-Maharlooei M, Li HW, Sykes M. T Cell Development and Responses in Human Immune System Mice. *Annu Rev Immunol.* 2024 Dec 20. Epub ahead of print.

8 Nikolic, B. *et al.* Normal development in porcine thymus grafts and specific tolerance of human T cells to porcine donor MHC. *J.Immunol.* **162**, 3402-3407 (1999).

9 Shimizu, I., Fudaba, Y., Shimizu, A., Yang, Y. G. & Sykes, M. Comparison of human T cell repertoire generated in xenogeneic porcine and human thymus grafts. *Transplantation* **86**, 601-610(2008).

10 Khosravi Maharlooei, M. H., M.; Li,H.; Vecchione,A.; Misra,A.; Madley,R.; Zhao,G.; Sykes,M. Generation of human/pig hybrid thymus to achieve immune tolerance to pig antigens with optimal immune function. *Xenotransplantation* **24**, 15 (2017).

11 Kalscheuer, H. O., T.; Dahmani,A.; Li,H.; Holzl,M.; Yamada, K.; Sykes,M. Xenograft tolerance and immune function of human T cells developing in pig thymus xenografts. *Journal of immunology* **192**, 3442-3450 (2014).

12 Khosravi-Maharlooei, M. *et al.* Rapid thymectomy of NSG mice to analyze the role of native and grafted thymi in humanized mice. *European journal of immunology* **50**, 138-141 (2020).

13 Weinstein, J. S., Hernandez, S. G. & Craft, J. T cells that promote B-Cell maturation in systemic autoimmunity. *Immunological reviews* **247**, 160-171 (2012).

14 Lang, J. *et al.* Studies of lymphocyte reconstitution in a humanized mouse model reveal a requirement of T cells for human B cell maturation. *Journal of immunology* **190**, 2090-2101 (2013).

15 Danner, R. *et al.* Expression of HLA class II molecules in humanized NOD.Rag1KO.IL2RgcKO mice is critical for development and function of human T and B cells. *PloS one* **6**, e19826 (2011).

16 Suzuki, M. *et al.* Induction of human humoral immune responses in a novel HLA-DR-expressing transgenic NOD/Shi-scid/gammacnull mouse. *International immunology* **24**, 243-252 (2012).

17 Mouat, I. C., Goldberg, E. & Horwitz, M. S. Age-associated B cells in autoimmune diseases. *Cellular and molecular life sciences: CMLS* **79**, 402 (2022).

18 Karnell, J. L. *et al.* Role of CD11c(+) T-bet(+) B cells in human health and disease. *Cellular immunology* **321**, 40-45 (2017).

19 Greenblatt, M. B. *et al.* Graft versus host disease in the bone marrow, liver and thymus humanized mouse model. *PloS one* **7**, e44664 (2012).

20 Lobo, P. I. Role of Natural Autoantibodies and Natural IgM Anti-Leucocyte Autoantibodies in

Health and Disease. *Frontiers in immunology* **7**, 198 (2016).
21 Verma, M. K. *et al.* A novel hemolytic complement-sufficient NSG mouse model supports studies of complement-mediated antitumor activity in vivo. *Journal of immunological methods* **446**, 47- 53 (2017).
22 Goldberg, B. S. & Ackerman, M. E. Antibody-mediated complement activation in pathology and protection. *Immunol Cell Biol* **98**, 305-317 (2020).
23 Brainard, D. M. *et al.* Induction of robust cellular and humoral virus-specific adaptive immune responses in human immunodeficiency virus-infected humanized BLT mice. *J.Virol.* **83**, 7305-7321 (2009).
24 Soloviova, K., Puliaiev, M., Foster, A. & Via, C. S. The parent-into-F1 murine model in the study of lupus-like autoimmunity and CD8 cytotoxic T lymphocyte function. *Methods in molecular biology* **900**, 253-270 (2012).
25 Tschetter, J. R., Mozes, E. & Shearer, G. M. Progression from acute to chronic disease in a murine parent-into-F1 model of graft-versus-host disease. *Journal of immunology* **165**, 5987-5994 (2000).
26 King, C., Ilic, A., Koelsch, K. & Sarvetnick, N. Homeostatic expansion of T cells during immune insufficiency generates autoimmunity. *Cell* **117**, 265-277 (2004).
27 Le Campion, A. *et al.* Lymphopenia-induced spontaneous T-cell proliferation as a cofactor for autoimmune disease development. *Blood* **114**, 1784-1793 (2009).
28 Zhang, N. & Bevan, M. J. TGF-beta signaling to T cells inhibits autoimmunity during lymphopenia- driven proliferation. *Nature immunology* **13**, 667-673 (2012).
29 McPherson, S. W., Heuss, N. D. & Gregerson, D. S. Lymphopenia-induced proliferation is a potent activator for CD4+ T cell-mediated autoimmune disease in the retina. *Journal of immunology* **182**, 969-979 (2009).
30 Onoe, T. *et al.* Homeostatic expansion and phenotypic conversion of human T cells depend on peripheral interactions with APCs. *Journal of immunology* **184**, 6756-6765 (2010).
31 Min, B., Yamane, H., Hu-Li, J. & Paul, W. E. Spontaneous and homeostatic proliferation of CD4 T cells are regulated by different mechanisms. *Journal of immunology* **174**, 6039-6044 (2005).
32 Surh, C. D. & Sprent, J. Homeostasis of naive and memory T cells. *Immunity* **29**, 848-862 (2008).
33 Tary-Lehmann, M., Lehmann, P., Schols, D., Roncarolo, M. G. & Saxon, A. Anti-SCID mouse reactivity shapes the human CD4+ T cell repertoire in hu-PBL-SCID chimeras. *J.Exp.Med.* **180**, 1817-1827 (1994).
34 Walker, L. S. K. The link between circulating follicular helper T cells and autoimmunity. *Nature reviews. Immunology* **22**, 567-575 (2022).
35 Yoshitomi, H. & Ueno, H. Shared and distinct roles of T peripheral helper and T follicular helper cells in human diseases. *Cellular & molecular immunology* **18**, 523-527 (2021).
36 Jenks, S. A., Cashman, K. S., Woodruff, M. C., Lee, F. E. & Sanz, I. Extrafollicular responses in humans and SLE. *Immunological reviews* **288**, 136-148 (2019).
37 Lai, H. Y., Chou, T. Y., Tzeng, C. H. & Lee, O. K. Cytokine profiles in various graft-versus-host disease target organs following hematopoietic stem cell transplantation. *Cell Transplant* **21**, 2033-2045 (2012).
38 Verlaat, L. *et al.* Novel pre-clinical mouse models for chronic Graft-versus-Host Disease. *Frontiers in immunology* **13**, 1079921 (2022).
39 Porcheray, F. *et al.* Expansion of polyreactive B cells cross-reactive to HLA and self in the blood of a patient with kidney graft rejection. *American journal of transplantation* **12**, 2088- 2097 (2012).

TABLE 1

Table 1: Mouse tissue-reactive human IgM and IgG in sera of HIS mice

			Pancreas	Liver	Spleen	Kidney	Thymus	SI	SG	Skin	AG	LI	Bone	Lung
Control Mouse	NSG	IgM	-	-	-	-	-	-	-	-	-	-	-	-
		IgG	-	-	-	-	-	-	-	-	-	-	-	-
Humanized, no thymus <20W	mouse #1	IgM	+	+	+	+	+	+	+	+	+	+	+	+
		IgG	-	-	-	-	-	-	-	-	-	-	-	-
	mouse #2	IgM	+	+	+	+	+	+	+	+	+	+	+	+
		IgG	-	-	-	-	-	-	-	-	-	-	-	-
Mouse Thymus <20W	mouse #3	IgM	+	+	+	+	+	+	+	+	+	+	+	+
		IgG	-	-	-	-	-	-	-	-	-	-	-	-
	mouse #4	IgM	+	+	+	+	+	+	+	+	+	+	+	+
		IgG	-	-	-	-	-	-	-	-	-	-	-	-
	mouse #5	IgM	+	+	+	+	+	+	+	+	+	+	+	+
		IgG	+	+	+	+	+	+	+	+	+	+	+	+
Mouse Thymus >30W	mouse #6	IgM	+	+	+	+	+	+	+	+	+	+	+	+
		IgG	+	-	-	+	+	+	-	+	-	+	+	+
	mouse #7	IgM	+	+	+	+	+	+	+	+	+	+	+	+
		IgG	-	-	-	-	-	-	-	-	-	-	-	-
	mouse #8	IgM	+	+	+	+	+	+	+	+	+	+	+	+
		IgG	-	-	-	-	-	-	-	-	-	-	-	-
Human Thymus >30W	mouse #9	IgM	+	+	+	+	+	+	+	+	+	+	+	+
		IgG	-	-	-	-	-	-	-	-	-	-	+	-
	mouse #10	IgM	+	+	+	+	+	+	+	+	+	+	+	+
		IgG	-	-	-	-	-	-	-	-	-	-	-	-
	mouse #11	IgM	+	+	+	+	+	+	+	+	+	+	+	+
		IgG	-	-	-	-	-	-	-	-	-	-	-	-

TABLE 2

Table 2: GVHD scoring system to assess disease severity based on five parameters: weight loss, posture, activity, fur condition, and skin condition.

Parameter	Criteria	Score
Weight Loss	10–25% weight loss compared to baseline	1
	>25% weight loss compared to baseline	2
Posture	Slight kyphosis	0.5
	Obvious kyphosis	1
	Kyphosis	1.5
	Severe kyphosis	2
Activity	Decreased activity	0.5
	Stationary >50% of the time	1
	Moves when stimulated	1.5
	No movement	2
Fur Condition	Ventral ruffling	0.5
	Ventral line and slight back ruffling	1
	Ruffling >50% of the body	1.5
	Ruffling entire body and denuded skin	2
Skin Condition	Flaking of ears, tail, or paws	0.5
	Erythema in tail or anus, ear shriveling	1
	Open lesions	1.5
	Multiple open lesions	2

Figure 1

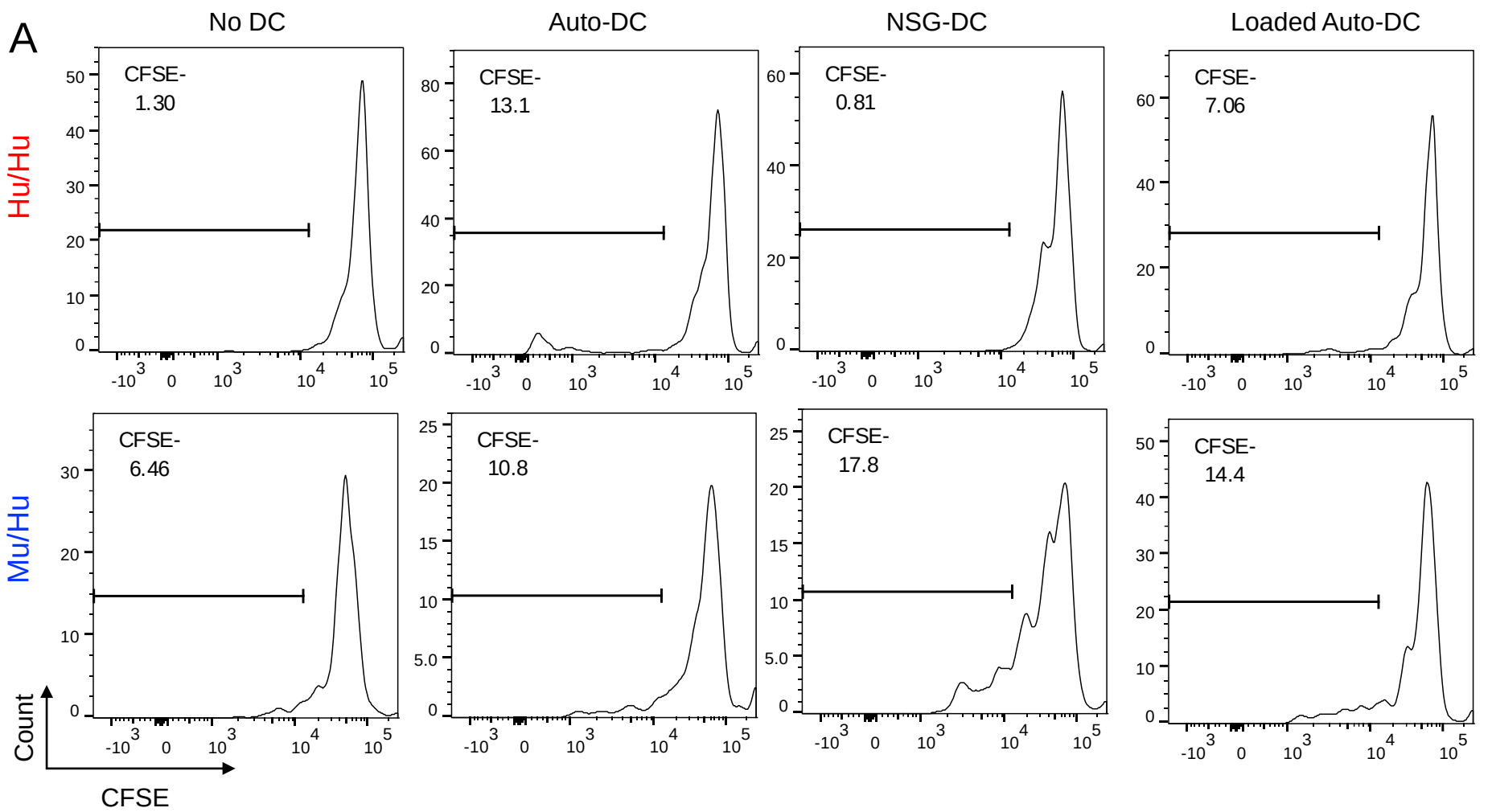
A
No DC
Auto-DC
NSG-DC
Loaded Auto-DC
Hu/Hu
Mu/Hu
CFSE-
1.30
CFSE-
13.1
CFSE-
0.81
CFSE-
7.06
CFSE-
6.46
CFSE-
10.8
CFSE-
17.8
CFSE-
14.4
Count
CFSE

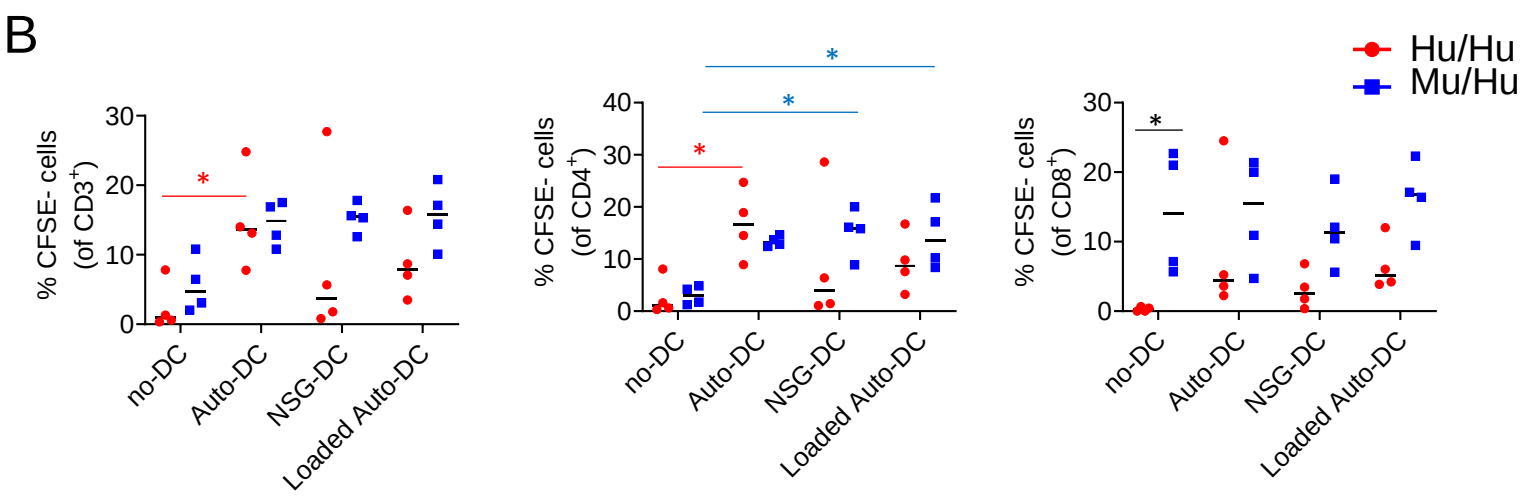
B
Hu/Hu
Mu/Hu
% CFSE- cells (of CD3+)
% CFSE- cells (of CD4+)
% CFSE- cells (of CD8+)
no-DC
Auto-DC
NSG-DC
Loaded Auto-DC

Figure 2

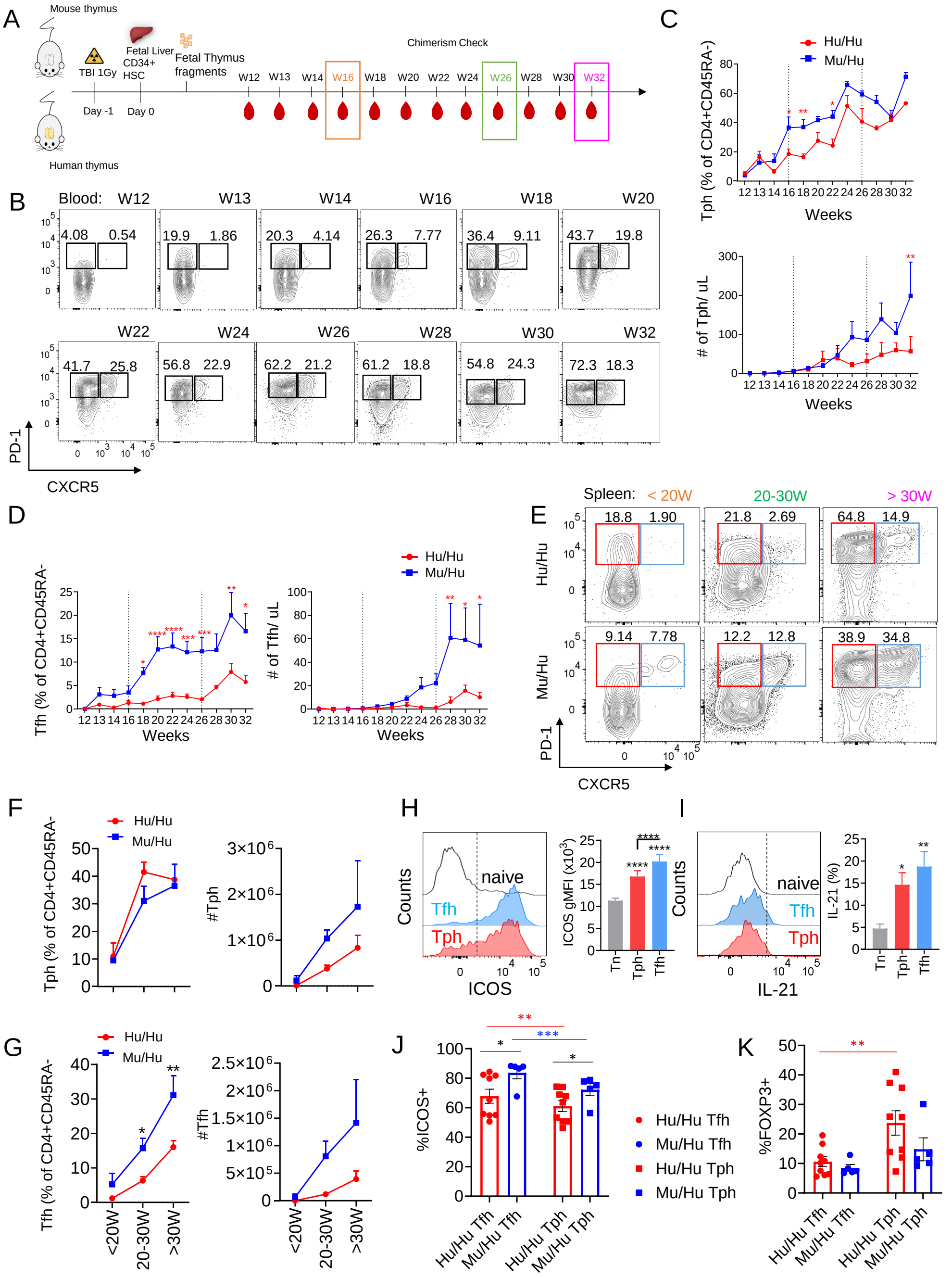
A
Mouse thymus
Human thymus
TBI 1Gy
Fetal Liver CD34+ HSC
Fetal Thymus fragments
Day -1
Day 0
Chimerism Check
W12 W13 W14 W16 W18 W20 W22 W24 W26 W28 W30 W32
B
Blood: W12 W13 W14 W16 W18 W20
4.08 0.54
19.9 1.86
20.3 4.14
26.3 7.77
36.4 9.11
43.7 19.8
W22 W24 W26 W28 W30 W32
41.7 25.8
56.8 22.9
62.2 21.2
61.2 18.8
54.8 24.3
72.3 18.3
PD-1
CXCR5
C
Hu/Hu
Mu/Hu
Tph (% of CD4+CD45RA-)
Weeks
# of Tph/ uL
Weeks
D
Hu/Hu
Mu/Hu
Tfh (% of CD4+CD45RA-)
Weeks
# of Tfh/ uL
Weeks
E
Spleen: < 20W 20-30W > 30W
18.8 1.90
21.8 2.69
64.8 14.9
9.14 7.78
12.2 12.8
38.9 34.8
Hu/Hu
Mu/Hu
PD-1
CXCR5
F
Hu/Hu
Mu/Hu
Tph (% of CD4+CD45RA-)
#Tph
H
Counts
naive
Tfh
Tph
ICOS
ICOS gMFI (x10^3)
Tn
Tph
Tfh
I
Counts
naive
Tfh
Tph
IL-21
IL-21 (%)
Tn
Tph
Tfh
G
Hu/Hu
Mu/Hu
Tfh (% of CD4+CD45RA-)
#Tfh
<20W
20-30W
>30W
J
%ICOS+
Hu/Hu Tfh
Mu/Hu Tfh
Hu/Hu Tph
Mu/Hu Tph
K
%FOXP3+
Hu/Hu Tfh
Mu/Hu Tfh
Hu/Hu Tph
Mu/Hu Tph

Figure 3

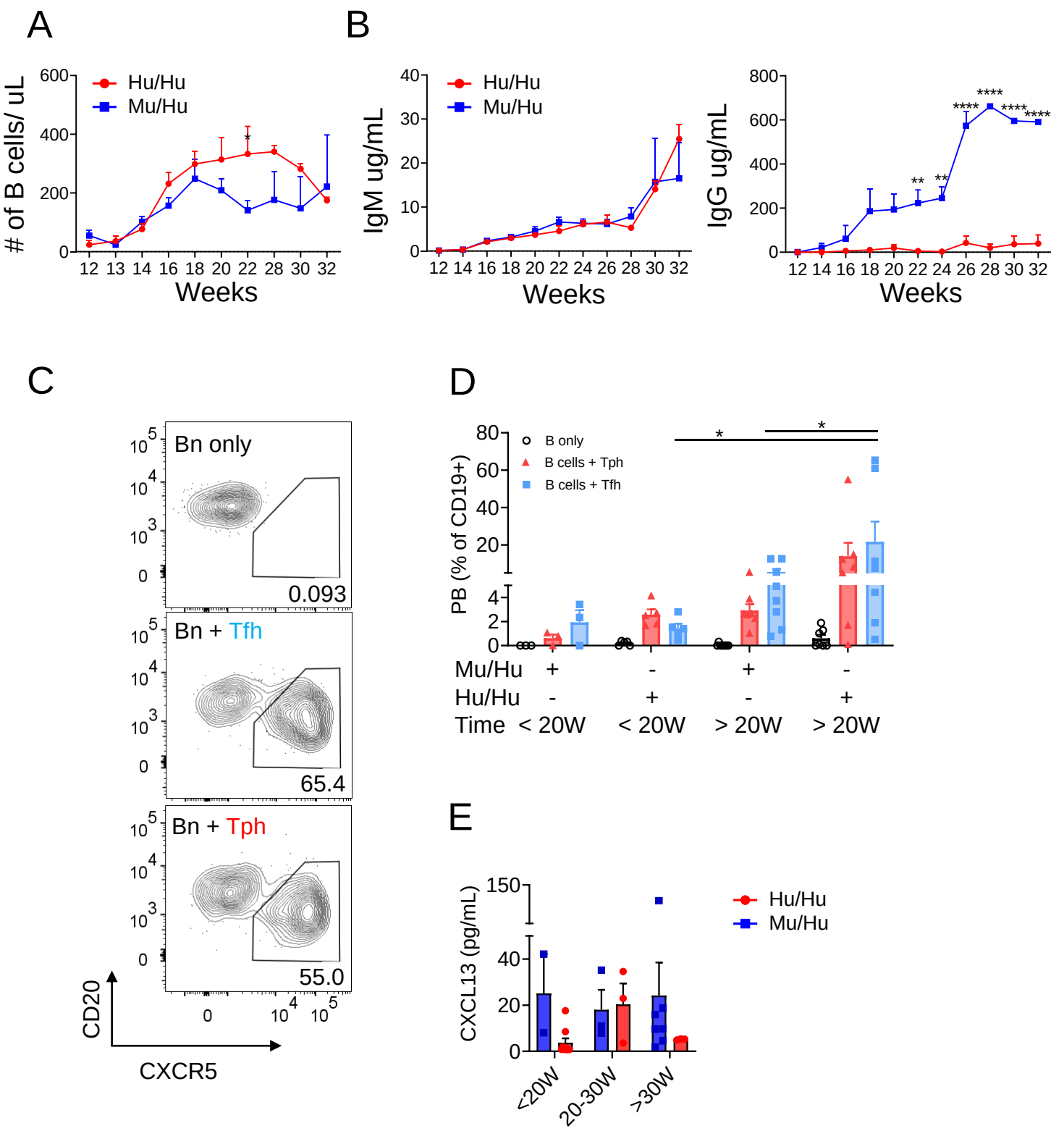
A
# of B cells/ uL
Hu/Hu
Mu/Hu
Weeks
B
IgM ug/mL
IgG ug/mL
Weeks
C
Bn only
0.093
Bn + Tfh
65.4
Bn + Tph
55.0
CD20
CXCR5
D
PB (% of CD19+)
B only
B cells + Tph
B cells + Tfh
Mu/Hu
Hu/Hu
Time
< 20W
> 20W
E
CXCL13 (pg/mL)
Hu/Hu
Mu/Hu
<20W
20-30W
>30W

Figure 4

A

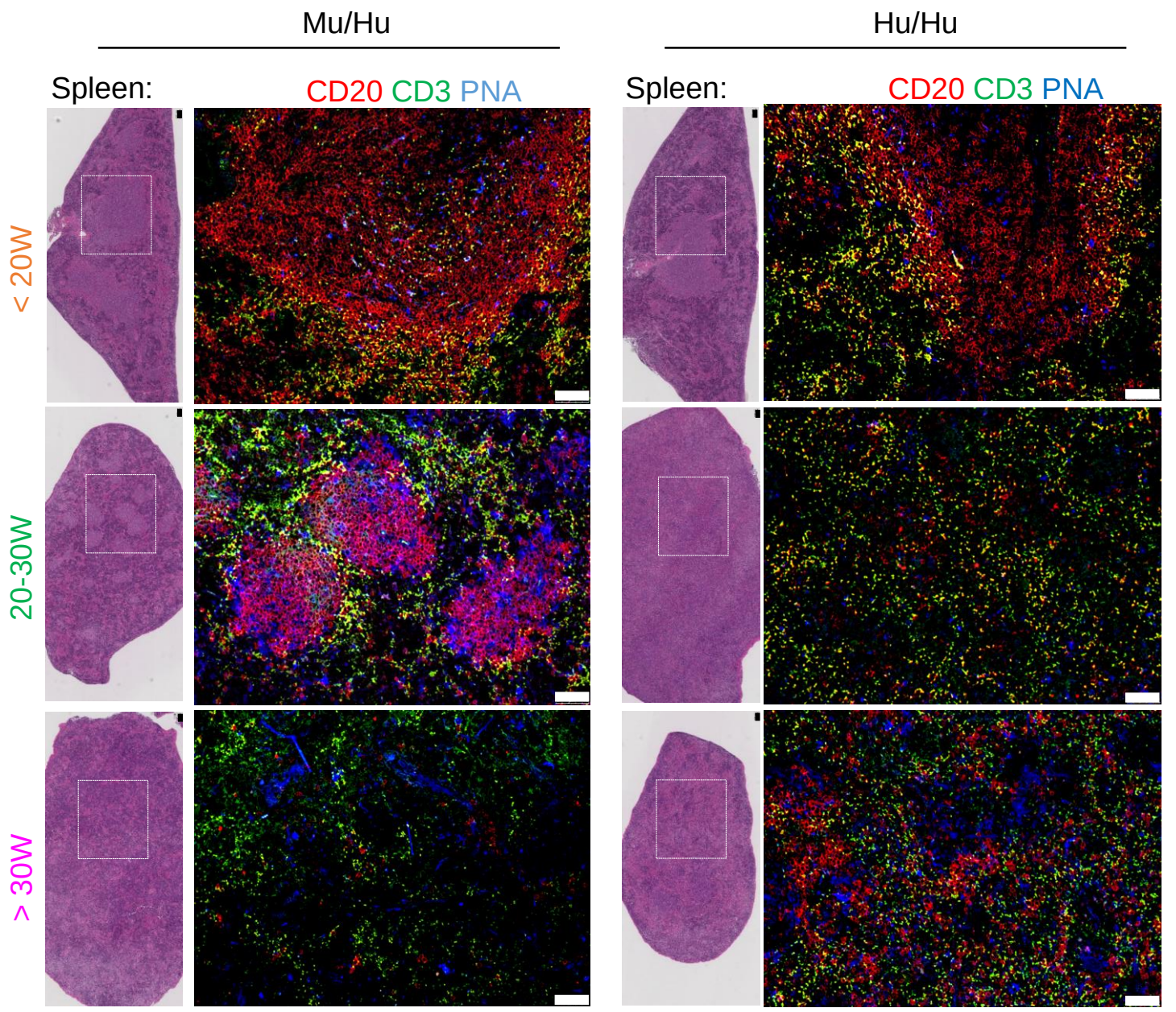
Mu/Hu
Hu/Hu
Spleen:
CD20 CD3 PNA
Spleen:
CD20 CD3 PNA
< 20W
20-30W
> 30W

B

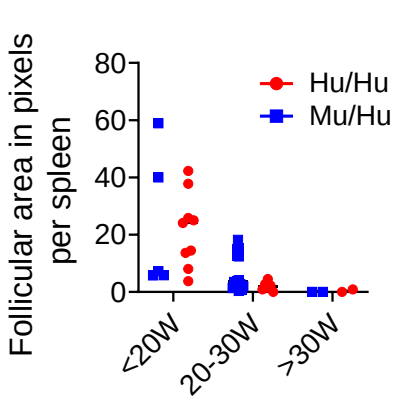
Follicular area in pixels per spleen
80
60
40
20
0
Hu/Hu
Mu/Hu
<20W
20-30W
>30W

C

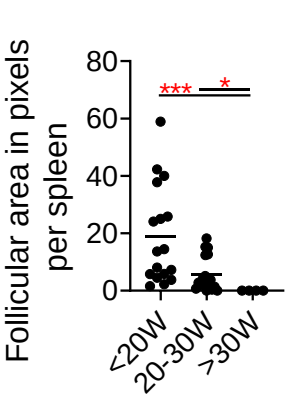
Follicular area in pixels per spleen
80
60
40
20
0
***
*
<20W
20-30W
>30W

Figure 5

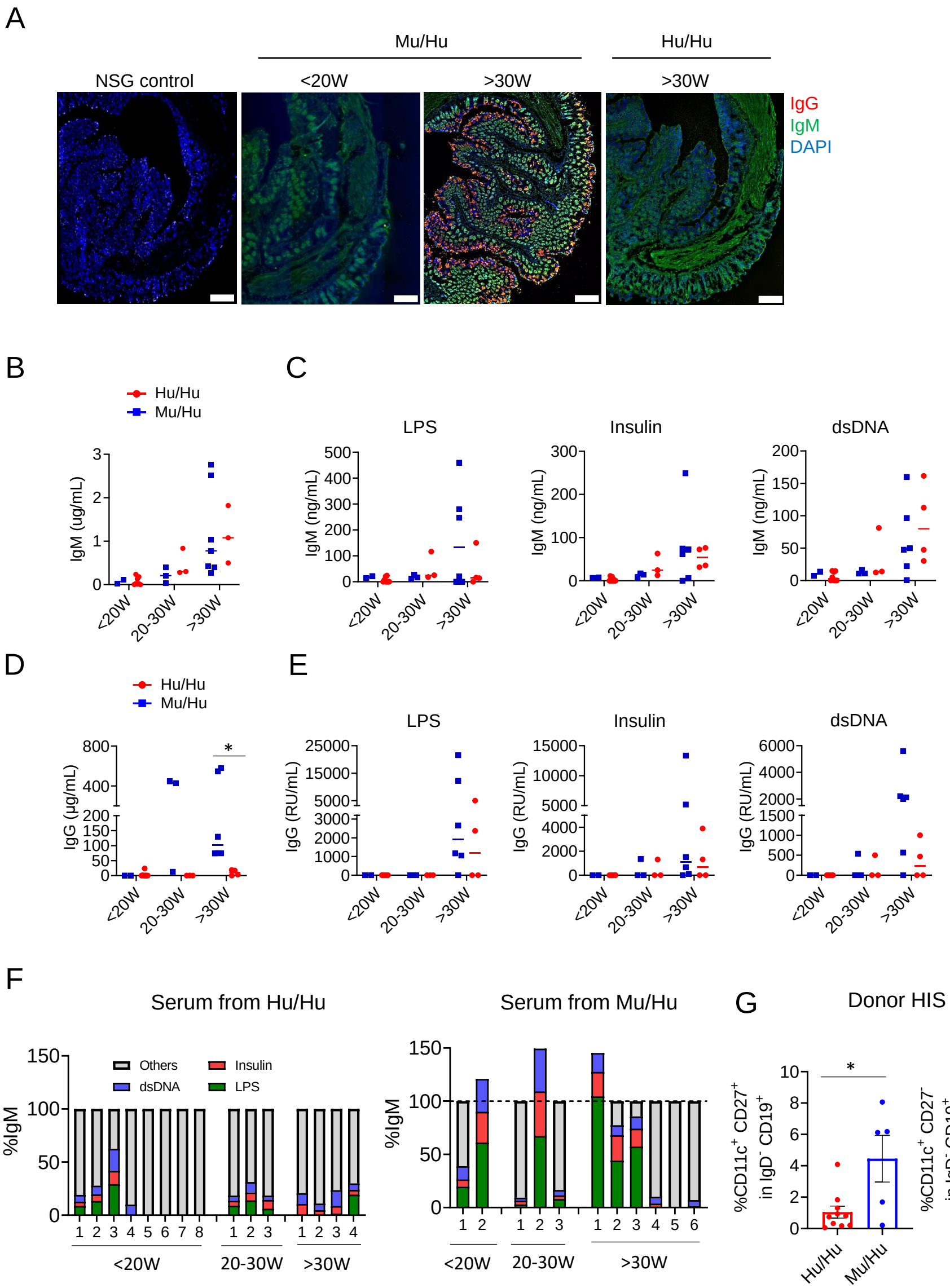
A
Mu/Hu
Hu/Hu
NSG control
<20W
>30W
>30W
IgG
IgM
DAPI
B
Hu/Hu
Mu/Hu
IgM (ug/mL)
<20W
20-30W
>30W
C
LPS
Insulin
dsDNA
IgM (ng/mL)
D
IgG (µg/mL)
E
IgG (RU/mL)
F
Serum from Hu/Hu
Serum from Mu/Hu
%IgM
Others
Insulin
dsDNA
LPS
G
Donor HIS mice
%CD11c+ CD27+ in IgD- CD19+
%CD11c+ CD27- in IgD- CD19+

Figure 6

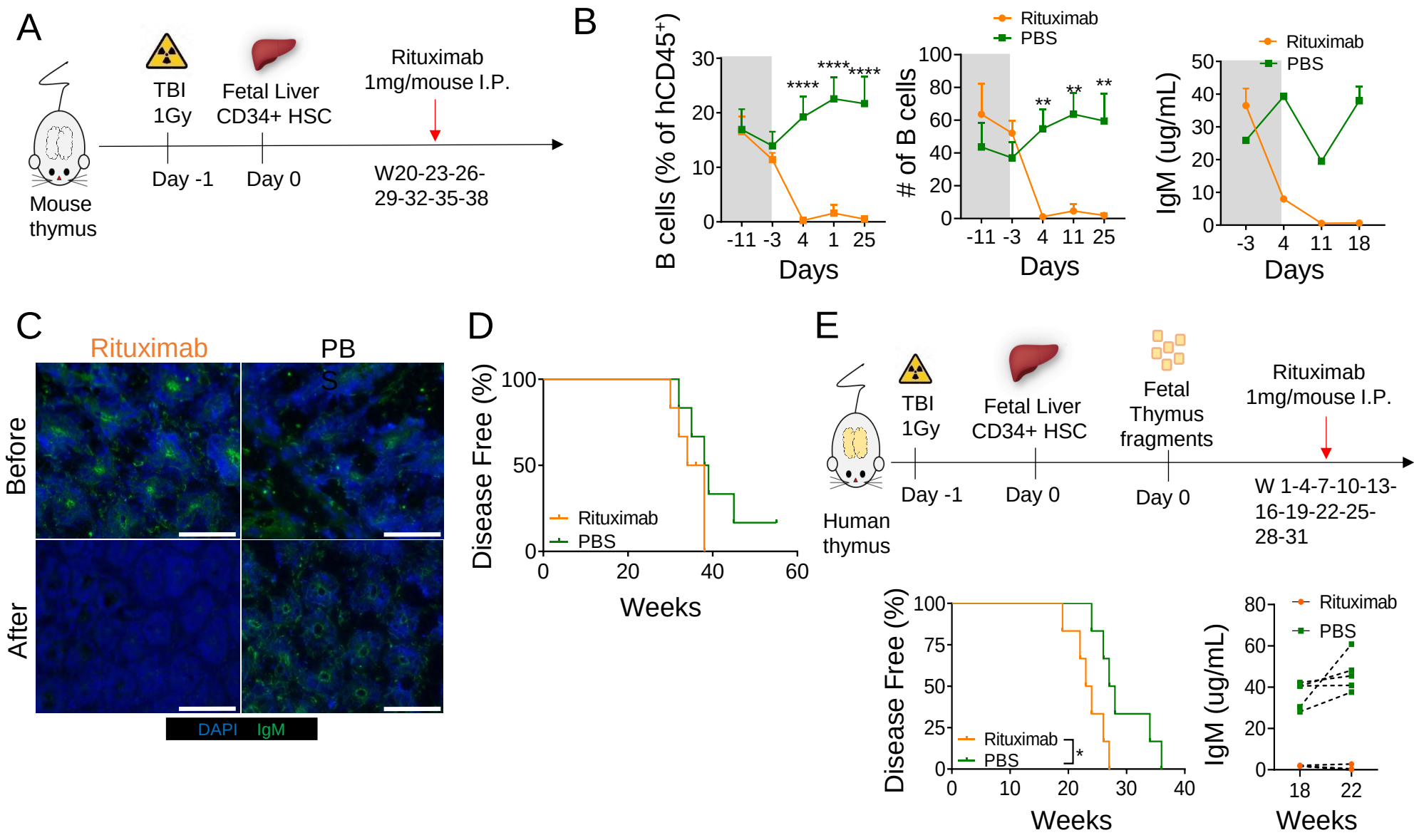
A
Mouse thymus
TBI 1Gy
Fetal Liver CD34+ HSC
Rituximab 1mg/mouse I.P.
Day -1
Day 0
W20-23-26-29-32-35-38
B
B cells (% of hCD45+)
Days
Rituximab
PBS
# of B cells
IgM (ug/mL)
C
Rituximab
PB
Before
After
DAPI IgM
D
Disease Free (%)
Weeks
E
Human thymus
TBI 1Gy
Fetal Liver CD34+ HSC
Fetal Thymus fragments
Rituximab 1mg/mouse I.P.
Day -1
Day 0
Day 0
W 1-4-7-10-13-16-19-22-25-28-31

Figure 7

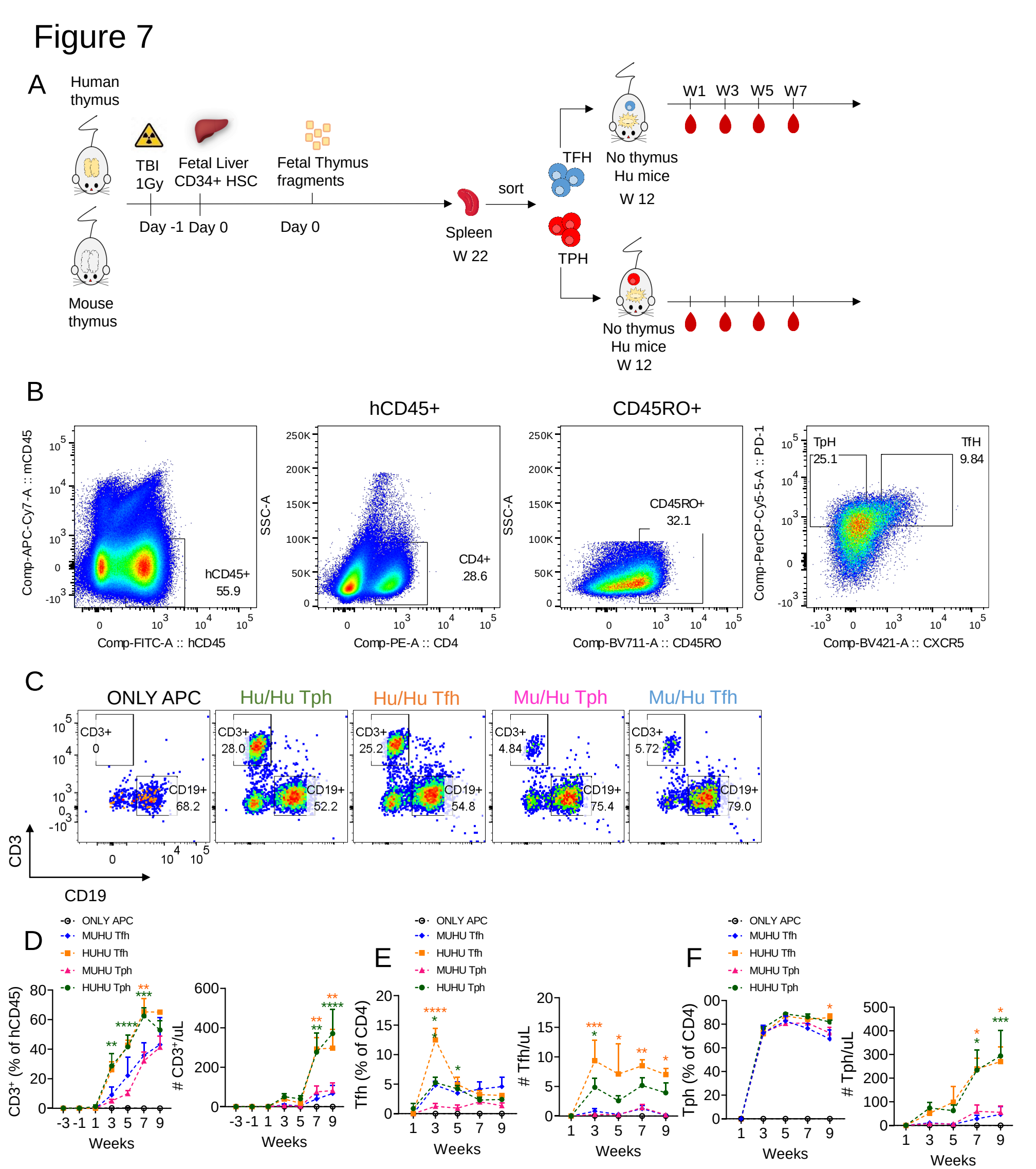
A
Human thymus
Mouse thymus
TBI 1Gy
Fetal Liver CD34+ HSC
Fetal Thymus fragments
Day -1 Day 0
Day 0
Spleen
W 22
sort
TFH
TPH
No thymus Hu mice
W 12
W1 W3 W5 W7
B
hCD45+
CD45RO+
Comp-APC-Cy7-A :: mCD45
Comp-FITC-A :: hCD45
hCD45+
55.9
SSC-A
Comp-PE-A :: CD4
CD4+
28.6
Comp-BV711-A :: CD45RO
CD45RO+
32.1
Comp-PerCP-Cy5-5-A :: PD-1
Comp-BV421-A :: CXCR5
TpH
25.1
TfH
9.84
C
ONLY APC
Hu/Hu Tph
Hu/Hu Tfh
Mu/Hu Tph
Mu/Hu Tfh
CD3+
0
CD19+
68.2
CD3+
28.0
CD19+
52.2
CD3+
25.2
CD19+
54.8
CD3+
4.84
CD19+
75.4
CD3+
5.72
CD19+
79.0
CD3
CD19
D
E
F
ONLY APC
MUHU Tfh
HUHU Tfh
MUHU Tph
HUHU Tph
CD3+ (% of hCD45)
CD3+/uL
Tfh (% of CD4)
Tfh/uL
Tph (% of CD4)
Tph/uL
Weeks

Figure 8

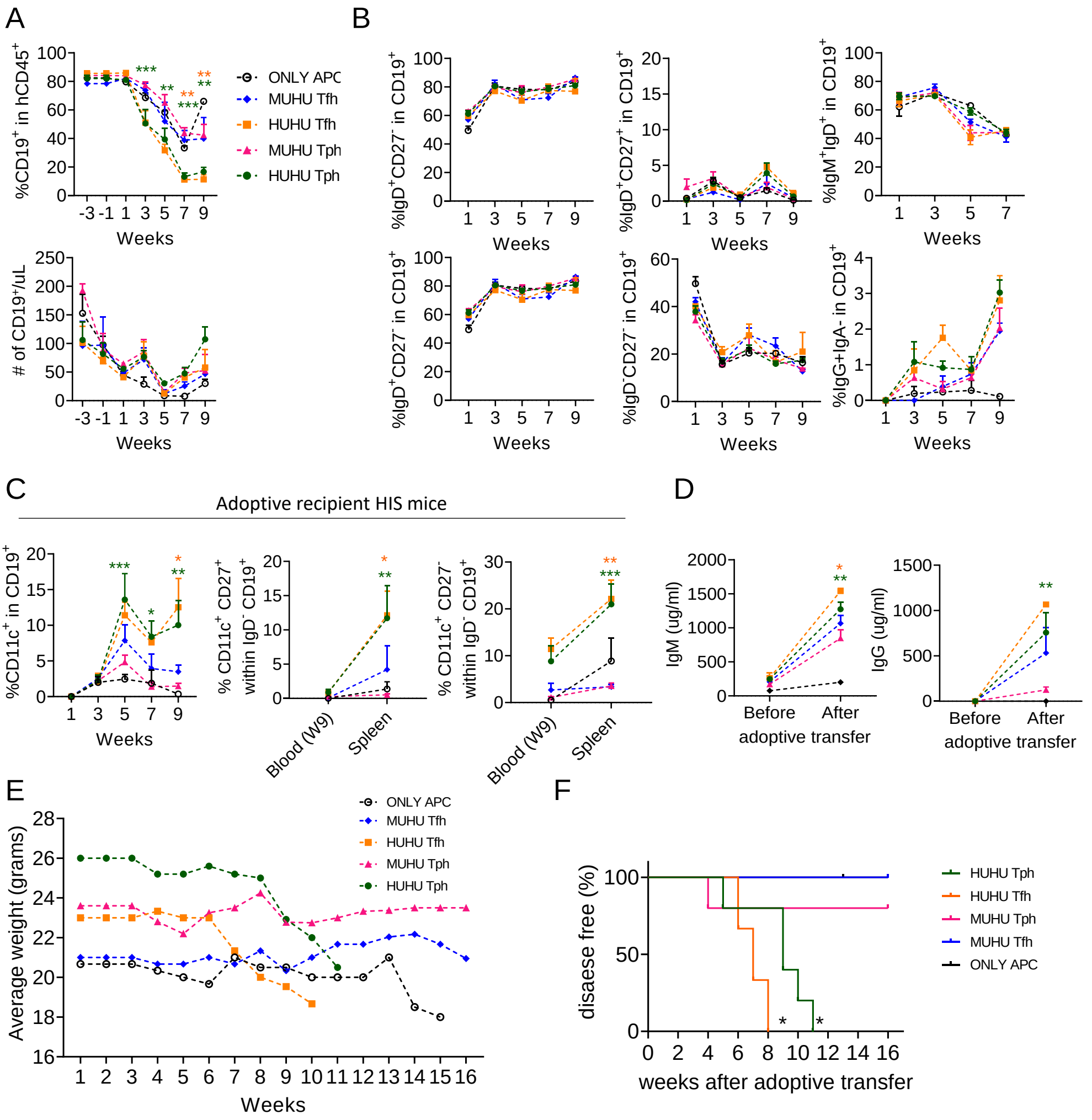
A
B
C
D
E
F
%CD19+ in hCD45+
# of CD19+/uL
Weeks
ONLY APC
MUHU Tfh
HUHU Tfh
MUHU Tph
HUHU Tph
%IgD+CD27- in CD19+
%IgD+CD27+ in CD19+
%IgM+IgD+ in CD19+
%IgD-CD27- in CD19+
%IgG+IgA- in CD19+
Adoptive recipient HIS mice
%CD11c+ in CD19+
% CD11c+ CD27+ within IgD- CD19+
% CD11c+ CD27- within IgD- CD19+
Blood (W9)
Spleen
IgM (ug/ml)
IgG (ug/ml)
Before adoptive transfer
After adoptive transfer
Average weight (grams)
disaese free (%)
weeks after adoptive transfer